Neurobiology of Disease 36 (2009) 494–508

Contents lists available at ScienceDirect

Neurobiology of Disease

journal homepage: www.elsevier.com/locate/ynbdi

Dopamine transporter glycosylation correlates with the vulnerability of midbrain dopaminergic cells in Parkinson's disease

Domingo Afonso-Oramas [a], Ignacio Cruz-Muros [a,d], Diego Álvarez de la Rosa [b], Pedro Abreu [c], Teresa Giráldez [e], Javier Castro-Hernández [a], Josmar Salas-Hernández [a], José L. Lanciego [d,f], Manuel Rodríguez [c,d], Tomas González-Hernández [a,d,*]

[a] Departamento de Anatomía, Facultad de Medicina, Universidad de La Laguna, Tenerife, Spain
[b] Departamento de Farmacología, Facultad de Medicina, Universidad de La Laguna, Tenerife, Spain
[c] Departamento de Fisiología, Facultad de Medicina, Universidad de La Laguna, Tenerife, Spain
[d] Centro de Investigación Biomédica en Red de Enfermedades Neurodegenerativas, Instituto de Salud Carlos III, Spain
[e] Unidad de Investigación, Hospital Universitario Ntra Sra de Candelaria, Tenerife, Spain
[f] Centro de Investigación Médica Aplicada, Universidad de Navarra, Spain

ARTICLE INFO

Article history:
Received 29 June 2009
Revised 3 September 2009
Accepted 7 September 2009
Available online 17 September 2009

Keywords:
Parkinson's disease
Pathogenesis
Dopamine transporter
Glycosylation
Differential vulnerability

ABSTRACT

The dopamine transporter (DAT) is a membrane glycoprotein responsible for dopamine (DA) uptake, which has been involved in the degeneration of DA cells in Parkinson's disease (PD). Given that DAT activity depends on its glycosylation status and membrane expression, and that not all midbrain DA cells show the same susceptibility to degeneration in PD, we have investigated a possible relationship between DAT glycosylation and function and the differential vulnerability of DA cells. Glycosylated DAT expression, DA uptake, and DAT V_{max} were significantly higher in terminals of nigrostriatal neurons than in those of mesolimbic neurons. No differences were found in non-glycosylated DAT expression and DAT K_m, and DA uptake differences disappeared after deglycosylation of nigrostriatal synaptosomes. The expression pattern of glycosylated DAT in the human midbrain and striatum showed a close anatomical relationship with DA degeneration in parkinsonian patients. This relationship was confirmed in rodent and monkey models of PD, and in HEK cells expressing the wild-type and a partially deglycosylated DAT form. These results strongly suggest that DAT glycosylation is involved in the differential vulnerability of midbrain DA cells in PD.

Introduction

Parkinson's disease (PD) is a neurodegenerative disorder characterized by neuronal degeneration and the presence of Lewy bodies in different brain areas (Braak et al., 2003; Burke et al., 2008). Genetic and environmental factors have been involved in its aetiology (Elbaz and Moisan, 2008; Lee and Liu, 2008), but the cause and many aspects of its pathogenesis are still unknown (Jenner and Olanow, 2006). Two important facts in PD are the loss of midbrain dopaminergic (DA−) neurons and the decline of dopamine (DA) in the striatum, which are responsible for most, if not all, motor symptoms (Foix and Nicolescom, 1925; Hassler, 1938). Numerous studies indicate that oxidative stress plays a central role in PD, and that DA metabolism is the main source of reactive oxygen species in DA cells (Luo and Roth, 2000; Adams et al., 2001). Therefore, DA may be responsible for DA cell degeneration in addition to being the neurotransmitter whose deficit characterizes PD. The cytosolic levels of DA depend on its synthesis, whose rate-limiting enzyme is tyrosine hydroxylase (TH), and two transport processes: DA uptake from the synaptic cleft, and once inside the cell, DA packing into small synaptic vesicles. DA uptake is performed by the dopamine transporter (DAT), a 12-transmembrane domain glycoprotein with three N-glycosylation sites in the second extracellular loop (Horn, 1990; Giros and Caron, 1993), which is also required for the cytotoxic effect of DA analogue neurotoxins (Blum et al., 2001; Schober, 2004). DA vesicular storage is performed by the vesicular monoamine transporter (VMAT2), also present in other monoaminergic cells. So, DAT may contribute to the vulnerability of DA cells, serving as an entrance for DA, its metabolites, and analogue toxins (Pifl et al., 1993; Gainetdinov et al., 1997; Bezard et al., 1999), and VMAT2 may serve as a neuroprotective factor by sequestering these substances into vesicles and preventing the interaction with their catabolic enzymes (Miller et al., 1999; Caudle et al., 2008). An interesting fact in PD is that not all midbrain DA neurons show the same susceptibility to degeneration. Neurons in the

Abbreviations: DA, dopamine; dSt, dorsal striatum; glyco-DAT, glycosylated DAT form; non-glyco-DAT, non-glycosylated DAT form; SNcv, substantia nigra, caudoventral, and lateral region; SNrm, substantia nigra, rostromedial, and dorsal region; vSt, ventral striatum; VTA, ventral tegmental area.

* Corresponding author. Department of Anatomy, Faculty of Medicine, University of La Laguna, 38207 La Laguna, Tenerife, Spain. Fax: 34 922 660253.
E-mail address: tgonhern@ull.es (T. González-Hernández).

Available online on ScienceDirect (www.sciencedirect.com).

0969-9961/$ – see front matter © 2009 Elsevier Inc. All rights reserved.
doi:10.1016/j.nbd.2009.09.002

substantia nigra (SN, A9 DA cell group; Dahlström and Fuxe, 1964) are more vulnerable than those in the ventral tegmental area (VTA, A10 DA cell group). Within the SN, neurons lying in its ventrolateral and caudal region (SNcv) are more vulnerable than those in the rostromedial and dorsal region (SNrm) (German et al., 1989; Damier et al., 1999b). The finding of higher DAT mRNA levels in nigral DA cells than in those in the VTA has suggested a relationship between DAT mRNA levels and vulnerability (Cerruti et al., 1993; Uhl et al., 1994). More recently, we found that midbrain DA neurons with similar DAT mRNA levels show differences in DAT protein expression, with some DA cells containing high levels of DAT mRNA and very low levels of DAT protein. Our results also revealed that the topographic pattern of DA cell degeneration matches that of DAT protein expression rather than that of DAT mRNA expression, suggesting that differences in DAT post-transcriptional regulation may be involved in the differential vulnerability of midbrain DA cells (Gonzalez-Hernandez et al., 2004). It is known that glycosylation in general, and N-glycosylation in particular, play a determinant role in the folding, trafficking, and surface expression of membrane proteins (Lis and Sharon, 1993; Kukuruzinska and Lennon, 1998). *In vitro* studies show that DAT activity depends on its glycosylation status, with the glycosylated DAT form transporting DA more efficiently than the non-glycosylated form (Torres et al., 2003; Li et al., 2004). The aim of this study was to investigate possible differences in the constitutive expression of the glycosylated and non-glycosylated DAT forms between different subpopulations of mesostriatal DA cells and whether the glycosylation status of DAT is related to the differential vulnerability of midbrain DA cells in PD.

Materials and methods

Mesostriatal compartments

Taking into account the topographical distribution of mesostriatal projections (Fallon and Loughlin, 1982; Joel and Weiner, 2000) and their degeneration pattern in PD (Bernheimer et al., 1973; Hirsch et al., 1988; Damier et al., 1999b) and in monkey (Burns et al., 1983; German et al., 1992) and rodent (Hung and Lee, 1996; Rodriguez et al., 2001) models of PD, the mesostriatal system was divided into two compartments: nigrostriatal and mesolimbic. The nigrostriatal compartment is composed of DA cells in the caudoventrolateral region of the substantia nigra (SNcv) and their projections to the dorsal striatum (dSt), which show high susceptibility to degeneration. The mesolimbic compartment is composed of DA cells in the rostrodorsomedial region of the substantia nigra (SNrm) and the ventral tegmental area (VTA) and their projections to the ventral striatum, which show low susceptibility to degeneration.

In monkeys and humans, the SNcv corresponds to the ventral part of the substantia nigra pars compacta (SNC) described by Damier et al. (1999a) and Kubis et al. (2000); the SNrm corresponds to the dorsal part of the SNC, and the VTA, to the band of sparse TH cells lying between the medial third of the SNrm and the red nucleus. With respect to the striatal division, according to hodological criteria, and in agreement with Fallon and Loughlin, (1982), Joel and Weiner (2000), and Heimer (2003), we considered the dSt as being composed of the two dorsal thirds of the dorsal striatum, and the vSt as being composed of the nucleus accumbens and the ventral third of the dorsal striatum. In humans and monkeys, both components of the dSt, caudate and putamen, were analysed separately.

DAT antibodies

Different commercial antibodies aimed at different fragments of DAT were tested in sections and protein extracts from mouse, rat, monkey, and human brain for the study of DAT expression by immunohistochemistry and Western blot. In our hands, the best results were obtained with three of them (Fig. 1A, see also Cruz-Muros et al., 2009). A rabbit polyclonal antibody against amino acids 541–620 at the carboxy terminus of the human DAT (Santa Cruz Biotechnology, Santa Cruz, CA; sc-14002; Schott et al., 2006) which shares 91% homology with the same region of rat DAT and shows a solid band at 50 kDa and a faint band at ~80 kDa (Fig. 1A, lanes 1–3); a rabbit polyclonal antibody against an 18-amino acid fragment near the N-terminus of rat DAT (Chemicon, Temecula, CA; AB1591P) which shares 88% homology with the same region of human DAT and shows a solid band at ~80 kDa and a thinner band at 50 kDa (Fig. 1A, lane 4; see also Freed et al., 1995; Vaughan et al., 1996), and a rat monoclonal antibody against the N-terminus fragment of human DAT (Chemicon; MAB369) which shares 89% homology with the same region of rat DAT. This antibody was tested in a protein extract from mouse, monkey and human striatum, and a band at ~75 –80 kDa was detected (Fig. 1A, lanes 7–10; see also Miller et al., 1997). To test their immunostaining specificity, primary antibodies were preabsorbed overnight at 4 °C with an excess amount of their respective synthetic peptides (50 μg/ml diluted antiserum). This test resulted in negative staining (Fig. 1A, lane 6). Taking into account previous studies using photoaffinity labelling, enzymatic treatment, and immunological detection of DAT (Patel et al., 1993; Vaughan, 1995; Vaughan et al., 1996), we can suggest that the band detected at ~80 kDa corresponds to the glycosylated DAT form, and the one at 50 kDa, to the non-glycosylated form. To confirm this suggestion, samples were treated with the endoglycosidase *N*-glycanase (0.5 U/100 μg protein; Sigma, St. Louis, MO) and the exoglycosidase neuraminidase (10 mU/100 μg protein; Sigma) for 4 hours at 37 °C before electrophoresis (Lew et al., 1991; Li et al., 2004; Vaughan et al., 1996; Zaleska and Erecinska, 1987). This treatment resulted in the loss of labelling at 75–80 kDa together with an increase at 50 kDa (Fig. 1A, lanes 5 and 8). Bearing in mind their labelling pattern in Western blot and their signal/background labelling ratio in immunohistochemistry, MAB369 and sc-14002 antibodies were used for the detection of the glycosylated and non-glycosylated DAT forms respectively in immunohistochemistry, and AB1591P and sc-14002 antibodies for the detection of the glycosylated and non-glycosylated DAT forms, respectively, in Western blot.

Morphological study

The morphological study was performed in parkinsonian patients, in mouse, rat, and monkey models of PD, and in their respective controls (non-parkinsonian humans and sham-lesioned mice, rats, and monkeys). Human brains were obtained from the Department of Pathology of the University Hospital of La Laguna and from the Brain Bank of Navarra (Hospital de Navarra, Servicio Navarro de Salud, CIMA and CIBERNED). Written consent for autopsy was obtained, and the study was approved by the Human Ethics Committee of the University of La Laguna. Experimental protocols in mice, rats, and monkeys were also approved by the Ethical Committees of the University of La Laguna and University of Navarra and were in accordance with the European Communities Council Directive of 24 November 1986 (86/609/EEC) regarding the care and use of animals for experimental procedures. Human brains were obtained from 6 patients (4 men and 2 women; average age 63.2 ± 4.4 years) who died without history of drug abuse or neurological or psychiatric illness and from 4 patients who died with a diagnosis of idiopathic PD (3 men and 1 woman; average age 64.3 ± 6.2 years; see Table 1). Brains were removed after a post-mortem period of 16.3 ± 5.4 hours. In each case, the absence of degenerative or vascular disease or the diagnosis of PD were confirmed by pathological examination. Blocks containing the entire midbrain DAergic formation (from the mammillary bodies to the pons) and the striatum (from 2 cm rostral to 2 cm caudal to the anterior commissure) were transversely cut into two rostrocaudal halves, and each one was hemisected in the sagittal plane. The pieces

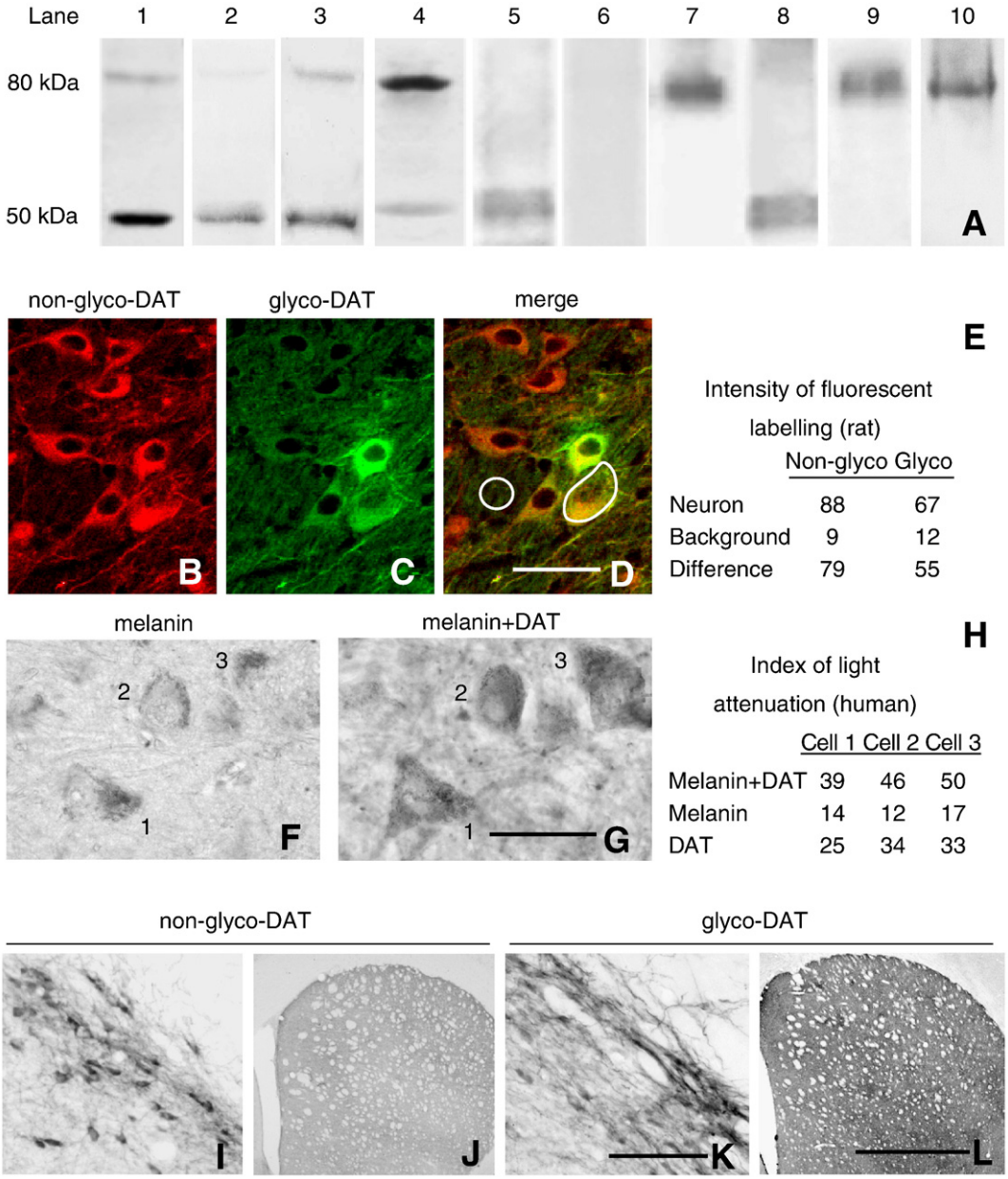

Fig. 1. Detection of glycosylated and non-glycosylated DAT forms by Western blot and immunostaining. (A) Western blot of whole protein extracts (70 μg) from rat (lanes 1, 4–6), mouse (lanes 7 and 8), monkey (lanes 2 and 9), and human (lanes 3 and 10) striata using different DAT antibodies: sc-14002 (lanes 1–3), AB1591P (lanes 4–6), and MAB369 (lanes 7–10). No staining was obtained after preabsorption of AB1591P with the immunogenic peptide (lane 6). Protein extracts were subjected to deglycosylation treatment before electrophoresis in lanes 5 and 8. We note that antibody sc-14002 (lanes 1–3) shows a solid band at 50 kDa, and antibodies AB1591P (lane 4) and MAB369 (lanes 7, 9, and 10) at 75 –80 kDa, and that after deglycosylation treatment, the molecular weight of the dense band detected with these two antibodies is reduced to 50 kDa (lanes 5 and 8). (B–H) Examples of densitometric analysis in rat and human midbrains using the antibody sc-14002, which detects the non-glycosylated DAT form (non-glyco-DAT; B), and the antibody MAB369, which detects the glycosylated DAT form (glyco-DAT; C). Double immunofluorescence was used in rats (B–D). Each DAT form was independently digitized, and after merging (D), they were analysed by separate channels (E). The circle in D indicates the neuropil region captured for the densitometric analysis of background. In humans (F–H), we used single immunohistochemistry for each DAT form. Three DA cells (1–3) were captured before (F) and after (G) DAT immunostaining in this example (see also Supplementary Fig. 1). Densitometric values of DAT immunostaining (H) result from subtracting labelling before immunostaining (melanin; F) from labelling after immunostaining (melanin + DAT; G). (I–L) Immunostaining for non-glyco-DAT (I and J) and glyco-DAT (K and L), using the antibodies sc-14002 and MAB369 respectively, in rat midbrain (I and K) and striatum (J and L). We note that non-glyco-DAT immunostaining is preferentially localized in DAergic cell somata, and glyco-DAT in fibres and terminals. Bar in D (for B–D), 20 μm; in G (for F and G), 25 μm; in K (for I and K), 100 μm; in L (for J and L), 1 mm.

were briefly washed in PBS and immersed in 4% paraformaldehyde in PBS for 72 hours at 4 °C. They were then cryoprotected in a graded series of sucrose–PBS solutions and stored at −80 °C until processing.

Animal models of PD

Ten male Sprague-Dawley rats (300–350 g), 10 male C57BL/6J mice (12–14 weeks of age, 24–28 g) and 6 male rhesus monkeys (*Macaca fascicularis*, 5–8 years old, 3.5–4.8 kg) were used in these experiments. Rats were injected in the third ventricle (midline, 2 mm posterior to bregma and 8 mm below the dura, according to Paxinos and Watson, 1998) with vehicle (0.9% saline solution with 0.3 μg/μl ascorbic acid, sham group, $n=5$) or a single dose (300 μg) of 6-OHDA (6-hydroxydopamine hydrochloride, Sigma; in 7.5 μl of vehicle per injection; 1 μl/min, 6-OHDA groups, $n=5$; for protocol details, see Rodriguez et al., 2001). Mice received four i.p. injections of 1-methyl-4-phenyl-1,2,3,6-tetrahydropyridine–HCl (MPTP, 20 mg/kg free base; Sigma) in saline ($n=5$) or saline alone ($n=5$) at 2 hour intervals (Jackson-Lewis et al., 1995). Rats and mice were sacrificed 7 days after

Table 1
Patient details.

Patients' no.	Diagnosis	Gender	Age at symptom onset (years)	Age of death (years)	Cause of death
1	Control	F	—	50	Ovarian cancer
2	Control	F	—	60	Renal failure
3	Control	M	—	72	Pneumonia
4	Control	M	—	65	Myocardial infarction
5	Control	M	—	57	Pancreatic cancer
6	Control	M	—	63	Aortic aneurysm
7	PD	F	59	67	Pneumonia
8	PD	M	51	61	Pulmonary embolism
9	PD	M	63	70	Pneumonia
10	PD	M	53	64	Pneumonia

F. female; M, male; PD, Parkinson's disease.

lesion. Parkinsonism was induced in the monkeys by weekly intravenous injections of 0.3–0.5 mg MPTP/kg. The progression of the parkinsonian syndrome was followed by using Unified Parkinson's Disease Rating Scale modified by Kurlan et al. (1991). MPTP injections were maintained until reaching a score of 15 points (range 0–29 points). Monkeys were considered as suffering a stable parkinsonism when they showed score fluctuations lower than 2 points during 2 months after MPTP withdrawn. Animals were deeply anaesthetised with an overdose of sodium pentobarbital and transcardially perfused with heparinized ice-cold 0.9% saline (15 ml in mice, 150 ml in rats, 1 l in monkeys) followed by 4% paraformaldehyde in PBS (50 ml in mice, 450 ml in rats, 3.5 l in monkeys). The brains were removed, and the midbrain and forebrain blocks were stored in the same fixative at 4 °C overnight, cryoprotected in a graded series of sucrose–PBS solutions, and stored at −80 °C until processing.

Tissue processing

Coronal sections (25 μm in mice and rats, 40 μm in monkeys, 50 μm in humans) were obtained with a freezing microtome, collected in parallel series, and processed for DAT and TH immunohistochemistry and Cresyl violet staining.

For single immunolabelling, floating sections were immersed for 30 minutes in 3% H_2O_2 to inactivate endogenous peroxidase, and incubated for 60 minutes at room temperature (RT) in 4% normal goat serum (NGS; Jackson ImmunoResearch, West Grove, PA) in PBS, containing 0.05% Triton X-100 (TX-100; Sigma), and overnight in PBS containing 2% NGS and one of the primary antibodies: rabbit anti-DAT polyclonal antibody (sc-14002; 1: 400), rat anti-DAT monoclonal antibody (MAB369; 1:800), or mouse anti-TH monoclonal antibody (Sigma, 1:12,000). After several rinses, the sections were incubated for 2 hours in either biotinylated goat anti-rabbit antiserum (1:1200; Jackson ImmunoResearch), biotinylated goat anti-rat antiserum (1:1200; Jackson ImmunoResearch), or biotinylated goat anti-mouse antiserum (1:1200; Jackson ImmunoResearch), respectively, and 1:200 NGS in PBS. Immunoreactions were visible after incubation for 1 hour at RT in ExtrAvidin–peroxidase (1:5000; Sigma) in PBS, and after 10 minutes in 0.005% 3′-3′-diamiobenzidine tetrahydrochloride (DAB; Sigma) and 0.001% H_2O_2 in cacodylate buffer 0.05N pH 7.6. Midbrain sections of the rats and striatal sections of the mice were also processed for double immunolabelling using both anti-DAT antibodies. After preincubation in 4% NGS and 0.05% Tx-100 in PBS, they were incubated overnight in rat anti-DAT monoclonal antibody (MAB369; 1:400) and rabbit anti-DAT polyclonal antibody (sc-14002; 1:200). Immunofluorescent labelling was visible after incubation for 3 hours in Cy2-conjugated goat anti-rat IgG (1: 150; Jackson ImmunoResearch) and Lissamine Rhodamine-conjugated goat anti-rabbit IgG (1: 150; Jackson ImmunoResearch) in PBS containing 1:200 NGS. After several rinses, the sections were mounted on gelatinized slides, air-dried, coverslipped with Vectashield (Vector), and examined under epifluorescence or confocal microscopy using appropriate filters.

Densitometric analysis

In order to quantify the relative expression levels of both DAT forms, a densitometric analysis was performed in midbrain DA somata of rats and humans and striatal terminals in monkeys and humans. In rat midbrains ($n=5$), the analysis was performed in double (glycosylated and non-glycosylated) immunofluorescent-stained sections (Figs. 1B–E). Different antibody and fluorophore dilutions were tested to establish the optimal work dilutions in the linear range of fluorescence intensity. All sections were processed simultaneously using the same protocol and chemical reagents, and all microscopic and computer parameters were kept constant throughout the densitometric study. In each rat, six sections 180 μm apart from each other in the rostrocaudal axis were randomly selected. In each section, the SNrm + VTA and SNcv were divided into fields of 300 μm × 250 μm, at a magnification of 200×. Only cell profiles including nucleus were analysed, and at least 60 cells per nucleus and rat were analysed. The labelling intensity of each cell was analysed individually using densitometry software (Leica Microsystems, Wetzlar, Germany). The image of each fluorochrome (Cy2 and Rhodamine) was digitised separately and then merged. Both fluorochromes were quantified simultaneously in separate channels. The labelling intensity of each fluorochrome was defined as the difference in fluorescent intensity (arbitrary units, range 0–255) between the cell and the neighbouring background (Fig. 1E).

In human midbrains ($n=4$), the densitometric analysis was performed in single immunostained sections. In each brain, 6 sections 1000 μm apart from each other and at least 100 cells per region were analysed. Bearing in mind that DA cells in human midbrains contain neuromelanin, the labelling intensity in immunostained cells arises in part from neuromelanin. In order to avoid the contribution of neuromelanin on densitometric values, its signal was subtracted in the following way. Semi-panoramic and high-magnification photographs were obtained from unstained sections. Taking advantage of the neuromelanin staining, individual DA cells were plotted and digitised (Fig. 1F and Supplementary Fig. 1A). After immunohistochemical processing, stained sections were photographed again (Fig. 1G and Supplementary Fig. 1B), and the densitometric value of each cell before processing (neuromelanin) was subtracted from the value found after processing (neuromelanin + immunostaining; Fig. 1H). Numerical data (labelling intensity) are expressed as the index of light attenuation in a 0 (white)–255 (black) range grey scale.

The labelling intensity of terminals was obtained from single immunostained sections in monkeys and humans. Twenty randomly selected square areas (0.5 mm × 0.5 mm in monkeys; 1 mm × 1 mm in humans) per region (caudate, putamen and vSt) and section ($n=5$) were analysed in each brain (monkeys, $n=4$; humans, $n=4$). The labelling intensity of each area was compared with that of the neighbouring corpus callosum or internal capsule.

Western blot analysis of DAT expression and DA uptake in rat striatal synaptosomes

The expression of the glyco- and non-glyco-DAT forms was also studied using Western blot analysis of total extracts of the ventral midbrain and the plasma membrane fraction of striatal synaptosomes of rats. The ventral midbrain (between 3.00 mm and 4.00 mm rostral to the interaural axis; Paxinos and Watson, 1998) and striatum (between 10.00 mm and 8.60 mm rostral to the interaural axis; Paxinos and Watson, 1998) were dissected from 6 freshly obtained rat brains using a brain blocker. The tissue was immediately placed on a cold plate and SNcv, SNrm + VTA, dSt, and vSt were dissected with the aid of a stereomicroscope and a scalpel for ophthalmic surgery (see

Gonzalez-Hernandez et al., 2004). Samples from each rat were processed and analysed separately. Whole midbrain protein extracts were obtained using the acid phenol method, resuspended in radioimmunoprecipitation assay (RIPA) lysis buffer pH 7.4, and quantified using the bicinchoninic acid method and bovine serum albumin as standard. In striata, synaptosomes and plasma membranes were obtained following the biochemical fractionation (Huttner et al., 1983; Dunah and Standaert, 2001) and impermeant biotinylation (Salvatore et al., 2003; Zhu et al., 2005) procedures. Samples were homogenized in 20 volumes of ice-cold sucrose bicarbonate solution (SBS, 320 mM sucrose in 5 mM sodium bicarbonate, pH 7.4) with 12 up and down strokes in a Teflon glass homogenizer. The homogenates were centrifuged (1000×*g*, 10 min, 4 °C), and the pellets (P1) containing nuclei and large debris were discarded. The supernatants (S1) were centrifuged (9200×*g*, 10 min, 4 °C), and the resulting pellets (P2) were resuspended in 1.2 ml SBS. These samples were divided into four aliquots: 0.3 ml for plasma membrane biotinylation, 0.3 ml to obtain the membrane-enriched fraction by hypo-osmotic lysis treatment, 0.3 ml for WB of the total synaptosomal fraction, and 0.3 ml for DA uptake. They were centrifuged at 10,200×*g* for 15 min at 4 °C, and the resulting pellets (P2′) were retained as crude synaptosomal fractions.

For plasma membrane biotinylation, synaptosomes (300 μg total protein) were incubated for 1 h at 4 °C with continual shaking in 500 μl of 1.5 mg/ml sulfo-NHS-biotin (Pierce, Rockford, IL) in PBS/Ca/Mg buffer (138 mM NaCl, 2.7 mM KCl, 1.5 mM KH_2PO_2, 9.6 mM Na_2HPO_4, 1 mM $MgCl_2$, 0.1 mM $CaCl_2$, pH 7.3) and centrifuged (8,000 g, 4 min, 4 °C). To remove biotinylating reagents, the resulting pellets were resuspended in 1 ml ice-cold 100 mM glycine in PBS/Ca/Mg buffer and centrifuged (8000×*g*, 4 min, 4 °C). The resuspension and centrifugation steps were repeated. Final pellets were resuspended again in 1 ml ice-cold 100 mM glycine in PBS/Ca/Mg buffer and incubated for 30 min at 4 °C. Samples were washed three further times in PBS/Ca/Mg buffer, and then lysed by sonication for 2–4 seconds in 300 μl Triton X-100 buffer (10 mM Tris, pH 7.4, 150 mM NaCl, 1 mM EDTA, 1% Triton X-100) containing protease inhibitors (1 μg/ml aprotinin, 1 μg/ml leupeptin, 1 mM pepstatin, 250 μM phenylmethylsulfonyl fluoride). After incubation in continuous shaking (30 min, 4 °C), the lysates were centrifuged (18,000×*g*, 30 min, 4 °C), and the supernatants were incubated with monomeric avidin bead–Triton X-100 buffer (100 μl) for 1 h at RT, and centrifuged (18,000×*g*, 4 min, 4 °C). The resultant supernatants (containing non-biotinylated intracellular proteins) were stored, and the pellets (containing avidin-absorbed biotinylated surface proteins) were resuspended in 1 ml Triton X-100 buffer and centrifuged (18,000×*g*, 4 min, 4 °C). Resuspension and centrifugation were repeated two more times, and the final pellets were stored.

To obtain plasma membrane-enriched fractions by hypo-osmotic lysis treatment, synaptosomes were transferred to a Teflon glass homogenizer, hypo-osmotically lysed by adding 9 volumes of ice-cold water, and subjected to three up and down strokes. The osmolarity of the lysates was restored by adding 1 M HEPES–NaOH pH 7.4 (final concentration, 7.5 mM HEPES–NaOH, pH 7.2), and the suspension was incubated in ice for 30 min. The homogenates were then centrifuged (25,000×*g*, 20 min, 4 °C) and the pellets (LP1) were stored.

For Western blot analysis, protein samples were diluted in Laemmli's loading buffer (62.5 mM Tris–HCl, 20% glycerol, 2% sodium dodecyl sulfate [SDS], 0.05% β-mercaptoethanol, and 0.05% bromophenol blue, pH 6.8), denatured (90 °C, 5 min), separated by electrophoresis in 10% SDS–polyacrylamide gel, and transferred to nitrocellulose (Schleicher & Schuell, Dassel, Germany). Blots were blocked for 2 hours at room temperature (RT) with 5% non-fat dry milk in TBST (250 mM NaCl, 50 mM Tris, pH 7.4, and 0.05% Tween20), and incubated overnight at 4 °C in blocking solution with one of the anti-DAT antibodies described above. After several rinses in TBST–5% milk, the membranes were incubated for 1 hour in horseradish peroxidase-conjugated anti-rabbit (1:10,000) or in horseradish peroxidase-conjugated anti-rat (1:10,000) IgG (Jackson ImmunoResearch, West Grove, PA). Immunoreactive bands were visualized using enhanced chemiluminescence (ECL; Amersham, Arlington, Heights, IL) and film exposure (Kodak Biomax, MR, Eastman Kodak, Rochester, NY). Different protein quantities, antibody dilutions, and exposure times were tested to establish the working range of each antibody and to ensure development within the linear range of the film. After DAT processing, each nitrocellulose membrane was subjected to stripping treatment (62.5 mM Tris, pH 6.8, 2% SDS, 100 mM β-mercaptoethanol; 1 hour at RT), and processed for tyrosine hydroxylase (Sigma; 1:10,000, overnight, 4 °C), or r-Actin using a mouse anti-r-Actin antibody (Sigma; 1:10,000, 2 hours at RT). The labelling densities for DAT were compared with those of TH and r-Actin by using a Bio-Rad scanner with densitometry software. A rectangle of uniform size and shape was placed over each band, and the density values were calculated by subtracting the background at approximately 2 mm above each band. The effectiveness of the subcellular fractionation was evaluated by using Syntaxin (mouse monoclonal anti-syntaxin, 1:500; Sigma) as a marker of synaptosomal membrane.

Synaptosomal [^{3}H]-DA uptake

[^{3}H]-DA uptake assays were performed by using freshly obtained synaptosomes from rat dorsal and ventral striata. To study the effect of DAT glycosylation on DA uptake, synaptosomal samples were exposed to deglycosylation treatment (neuraminidase 10 mU/100 μg protein (Sigma), *N*-glycanase 0.5 U/100 μg protein (Sigma), for 20 min, 34 °C) and analysed in parallel to untreated samples. Fifty microlitres of synaptosomal suspension (0.5 μg total protein/μl) was preincubated (30 °C, 5 min) with 25–1250 nM DA (Sigma; with or without 10 μM nomifensine; Sigma) in assay buffer (125 mM NaCl, 5 mM KCl, 1.5 mM $MgSO_4$, 1.25 mM $CaCl_2$, 1.5 mM KH_2PO_2, 10 mM glucose, 25 mM HEPES, 0.1 mM EDTA, 0.1 mM pargyline, and 0.1 mM ascorbic acid). Subsequently, 20 nM [^{3}H]-DA (final concentration; Amersham, Buckinghamshire, UK) was added to each tube. The total assay volume was 200 μl. After 10 min incubation at 30 °C, DA uptake was stopped by the addition of 200 μl ice-cold assay buffer. The suspension was immediately filtered under vacuum through MultiScreen®—0.45 μm hydrophilic filters (Millipore, Molsheim, France). The filters were washed twice with 200 μl ice-cold assay buffer, excised, and placed in scintillation vials containing 3 ml liquid scintillation Cocktail (Sigma) and stored overnight at room temperature. Accumulated radioactivity was quantified using a liquid scintillation counter (LKB Rackbeta 1214; Turku, Finland). Nonspecific uptake, defined as the DA uptake in the presence of nomifensine, was subtracted from total uptake to define DAT-mediated specific uptake. All assays were performed in triplicate. V_{max} and K_m values were determined by non-linear regression.

In vitro study

Plasmid constructs, mutagenesis, and cell line transfection

Rat DAT cDNA was used since previous studies show no differences in DA uptake and MPP^+ susceptibility between cells expressing human or rat DAT (Pifl et al., 1993). Full-length rat DAT cDNA was obtained by RT–PCR from mRNA extracted from rat substantia nigra using a proof-reading DNA polymerase (Expand High Fidelity Kit; Roche). Specific primers were designed from the reported sequence (GenBank accession number NM_012694) and specific restriction sites were added to the 5′- and 3′-ends to facilitate cloning. Primer sequences were as follows: rDAT-F: 5′-GGGGTACCCGCCACCATGAG-TAAGAGCAAATGCTCCGTG-3′and rDAT-R:5′-GGAATTCTTACAG-CAACAGCCAGTGACGCAG-3′. The amplified fragment was cloned in pcDNA3.1(+)-neomycin (Invitrogen). Point mutations targeting two

of the three N-glycosylation places (N188Q and N205Q) of the second extracellular loop (Torres et al., 2003; Li et al., 2004) were introduced by PCR with the QuickChange mutagenesis kit (Stratagene). Primer sequences were as follows (mutant nucleotides are indicated in lower case): N188QF: 5′-GCAACAACACCTGGAATtcC CCCcAgTGCTCCGATGCC-3′; N188QR: 5′-GGCATCGGAGCAcTgGGGGgaATTCCAGGTGTTGTTGC-3′; N205QF: 5′-CTAGCGACGGCCTaGGCCTCcAgGACACCTTTGGG-3′; and N205QR: 5′-CCCAAAGGTGTCcTgGAGGCCtAGGCCGTCGCTAG-3′. Silent mutations were used to introduce new restriction sites (*Eco*RI in N188Q and *Stu*I in N205Q) for rapid characterization of the mutants.

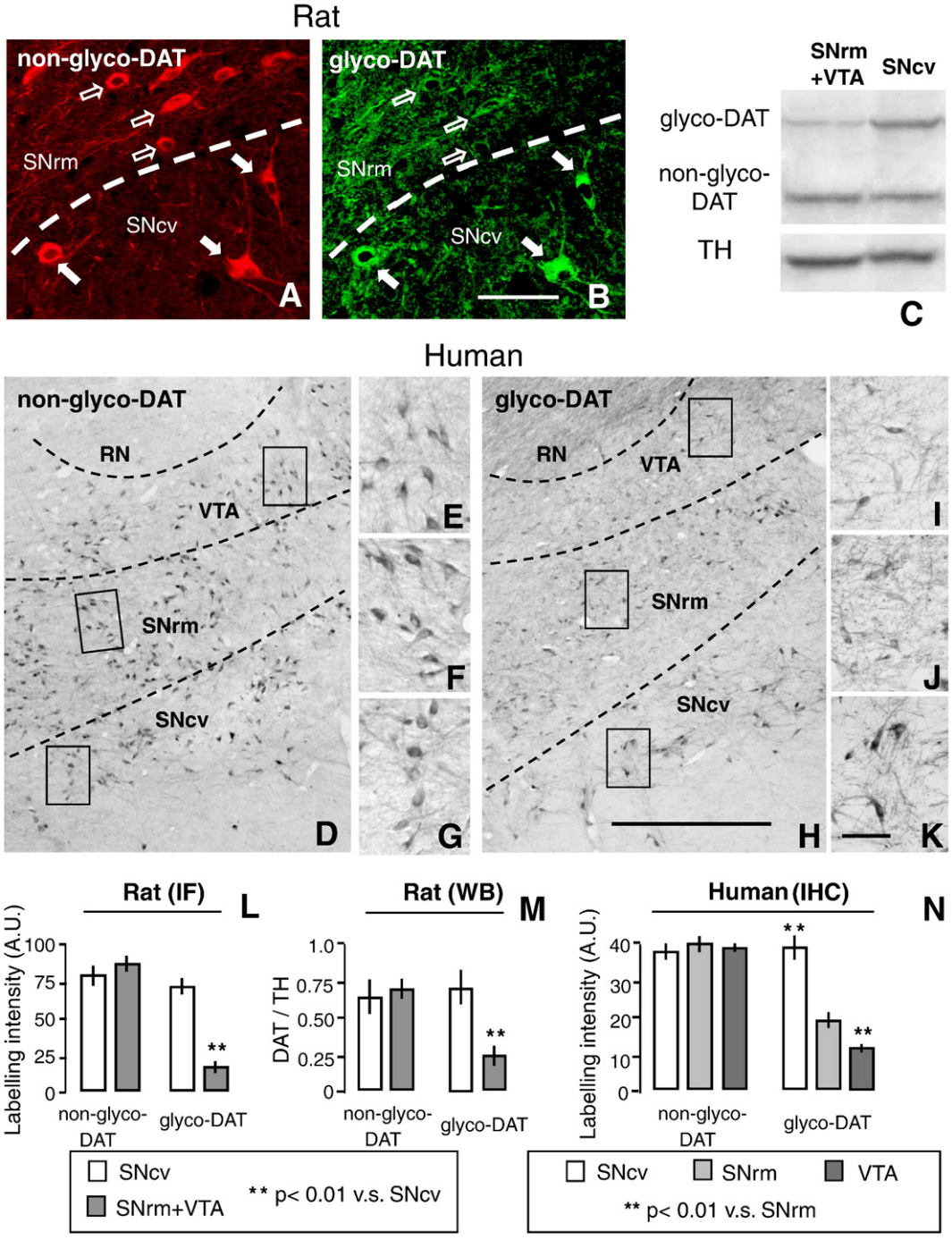

Fig. 2. Immunolabelling pattern and densitometric analysis of non-glyco- and glyco-DAT expression in the rat and human midbrain. (A and B) Double immunofluorescent staining of non-glyco-DAT (A) and glyco-DAT (B) in the rat substantia nigra. (C) Western blot analysis of non-glyco-DAT, glyco-DAT, and TH expression in the rat midbrain. (D–G) Immunohistochemistry for non-glyco-DAT in the human substantia nigra. (E–G) Correspond to the boxed areas at the top, in the middle and at the bottom of D, respectively. (H–K) Immunohistochemistry for glyco-DAT in the human substantia nigra. (I–K) Correspond to the boxed areas at the top, in the middle, and at the bottom of H, respectively. (L–N) Densitometric analysis of immunolabelling in rats (L) and humans (N), and Western blot in rats (M). AU, arbitrary units; DAT/TH, DAT expression with respect to TH expression; RN, red nucleus; SNcv, caudoventrolateral region of the substantia nigra; SNrm, rostrodorsomedial region of the substantia nigra; VTA, ventral tegmental area. The dashed lines in A, B, D, and H indicate the putative border between VTA and SNrm, and between SNrm and SNcv. Solid arrows in A and B indicate DA cells showing high expressions of both glyco- and non-glyco- DAT. Open arrows in A and B indicate DA cells showing a high expression of non-glyco-DAT and a low expression of glyco-DAT. We can see that the labelling intensity for non-glyco-DAT is similar in the SNrm, SNcv, and VTA in both rat (A) and human substantia nigra (D–G), while the labelling intensity for the glyco-DAT form is significantly higher in the SNcv than in the SNrm and VTA (B, H–K). These differences were confirmed by densitometry (L and N) and also evident in Western blot in rats (C and M). Bar in B (for A and B), 40 μm; in H (for D and H), 450 μm; in K (for E–G and I–K), 50 μm.

All constructs were sequenced at the University of La Laguna DNA sequencing facility.

HEK293 cells were maintained in Dulbecco's modified Eagle's medium (DMEM) supplemented with 10% fetal bovine serum, penicillin and streptomycin in a humidified incubator set at 37 °C and 5% CO_2. Cells were transfected with Lipofectamine 2000 (Invitrogen) following the manufacturer's instructions. Stable cell lines expressing wild-type or mutant rDAT were obtained by growth on selective medium containing 1 mg/ml of G418 (Invitrogen). After 10–12 days of selection in G418, individual clones were expanded in

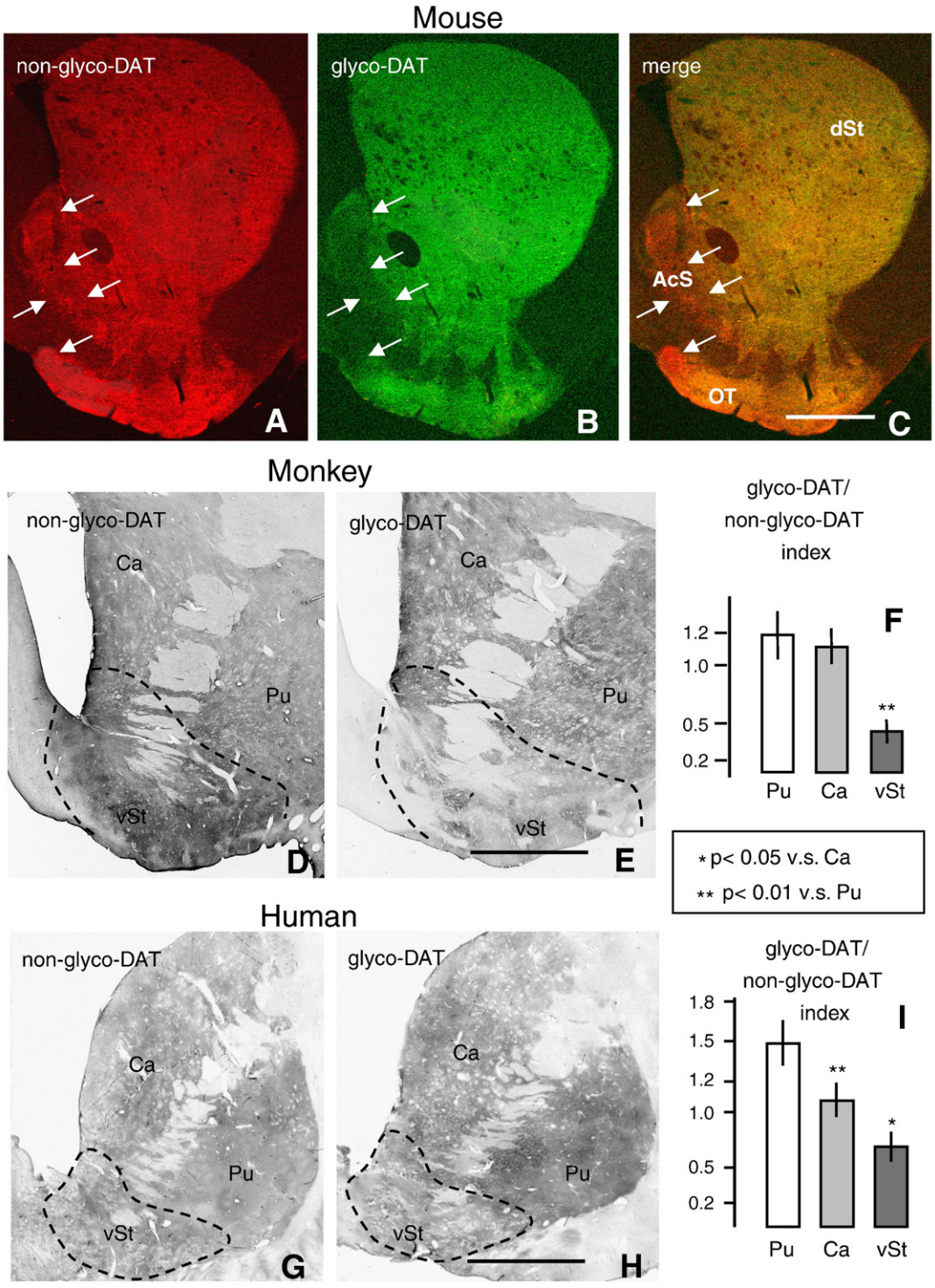

Fig. 3. Immunolabelling pattern and densitometric analysis of non-glyco- and glyco-DAT expression in the mouse (A–C), monkey (D–F), and human (G–I) striatum. AcS, accumbens shell; Ca, caudate nucleus; dSt, dorsal striatum; OT, olfactory tubercle; Pu, putamen; vSt, ventral striatum. The dashed line in D, E, G, and H indicates the putative borders of the vSt. Note that in mice, the labelling intensity for non-glyco-DAT is similar in the different striatal regions, while that for glyco-DAT is much lower in the AcS and the medial region of the OT (arrows in A–C) than in other striatal regions. As shown in immunohistochemistry (D, E) and densitometry (F), the labelling intensity for non-glyco-DAT in the monkey vSt is higher than that in the dSt (Ca and Pu), while that for glyco-DAT is lower than that in the dSt. In the human striatum, no regional differences were detected in non-glyco-DAT immunostaining (G), while the glyco-DAT labelling showed an intensity gradient (Pu>Ca>vSt; H and I). Bar in C (for A–C), 300 μm; in E (for D and E), 1.4 mm; in H (for G and H), 9 mm.

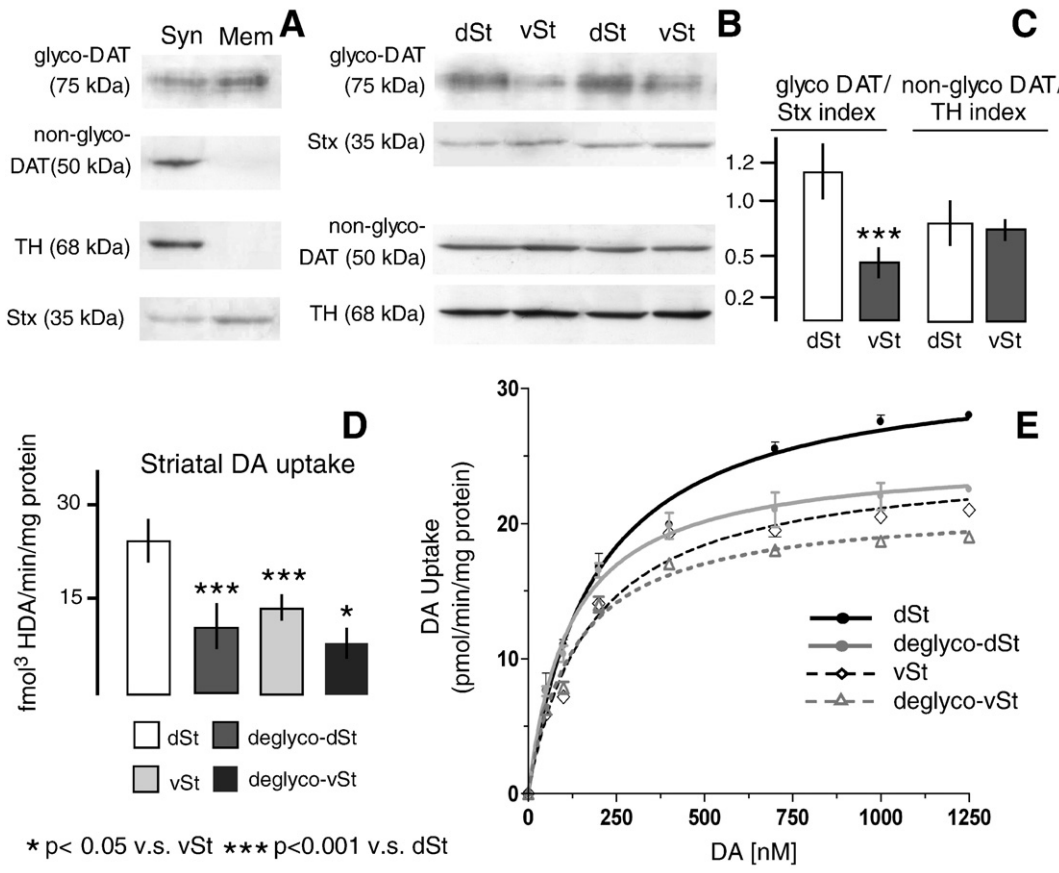

Fig. 4. DAT expression and DA uptake in striatal synaptosomes of rats. (A) Glyco-DAT and non-glyco-DAT expression in whole extracts (Syn) and plasma membranes (Mem) of striatal synaptosomes. Whole extracts contain both the non-glyco- and the glyco-DAT forms, while plasma membranes only contain the glycosylated DAT form. Syntaxin (Stx) was used as a marker of plasma membranes, and tyrosine hydroxylase (TH) as a marker of the non-plasma membrane compartment of dopaminergic terminals. (B and C) Expression of glyco-DAT in the plasma membrane of synaptosomes in the dorsal (dSt) and ventral (vSt) striatum. Glyco-DAT expression is higher in the plasma membrane of the dSt than in the vSt. No differences were detected in the expression of the non-glyco-DAT form in whole synaptosomal extracts. (D and E) DA uptake, kinetics of DA uptake, and effects of deglycosylation treatment. DA uptake in the dSt is two-fold higher than that in the vSt. Deglycosylation reduces DA uptake (D) and DAT kinetics (E) in both striatal regions. The calculated V_{max} and K_m are listed in Table 2.

multiwell plates and examined for DAT expression by Western blot and immunofluorescence. Several positive clones were identified and used for subsequent experiments.

[^{3}H]-DA uptake and cytotoxicity assays

DA uptake and cytotoxicity assays in HEK transfected cells were performed according to Storch et al. (2004) and Li et al. (2004). Wild-type and transfected cells were grown to confluence on 6-well dishes. They were dissociated with trypsin–EDTA, and after cell detaching, the trypsin action was immediately terminated by adding the same volume of DMEM. Cells were centrifuged at 1000 rpm for 2 min, washed twice and resuspended in assay buffer (125 mM NaCl, 5 mM KCl, 1.5 mM $MgSO_4$, 1.25 mM $CaCl_2$, 1.5 mM KH_2PO_2, 10 mM glucose, 25 mM HEPES, 0.1 mM EDTA, 0.1 mM pargyline, and 0.1 mM ascorbic acid). Samples of 50 µl cell suspensions (1 µg total protein/µl) were analysed as described for synaptosomes.

Cell vulnerability was analysed by using a MTT (3[4,5-dimethylthiazol-2-yl]-2,5-diphenyltetrazolium bromide) assay and two different neurotoxins: 1-methyl-4-phenylpyridine (MPP^+), the active metabolite of MPTP, whose toxicity depends on DAT activity, and rotenone, a lipophilic compound that crosses the cellular membranes without depending on the transporter (Uversky, 2004). Cells were seeded in 24-well dishes at a density of 20,000 cells/well (in 400 µl medium) and grown for 48 hours. The medium was then supplemented with ascorbic acid (0.022 mg/ml final concentration), and 24 hours later, different concentrations of either rotenone (0.1 – 1000 µM; Sigma) or MPP^+ (0.01 –1000 µM; Sigma) with and without nomifensine (17.7 µg/ml) were added. After incubation for 24 hours at 37 °C, 100 µl of MTT reagent (0.5% MTT in PBS, 0.1% final concentration) was added to each well and incubated at 37 °C for 3 hours. Thereafter, 400 µl of lysis buffer (20% wt./vol. sodium dodecyl sulfate (SDS) in 50% *N*,*N*-dimethyl formamide, with 2.5% HCl and 2.5% acetic acid, pH 4.7) was added and incubated overnight at 37 °C. The optical density of the samples was then measured at 570 nm with reference at 630 nm. MTT reduction was expressed as a percentage of the untreated wild-type HEK cells. The cytotoxic effect of MPP^+ was also analysed using morphological criteria. Taking into consideration the results in the MTT assay, cells were incubated for 24 hours in 50 µM MPP^+ with and without nomifensine. Thereafter, they were

Table 2
Kinetics of [^{3}H]-DA uptake in synaptosomes of the dorsal (dSt) and ventral (vSt) striatum of rats, and effect of deglycosylation treatment.

	dSt	vSt	deglyco-dSt	deglyco-vSt
V_{max}[a]	31.86 ± 1.03	24.53 ± 0.98*	24.93 ± 0.68*	21.33 ± 0.46**
K_m[b]	185.70 ± 14.10	177.10 ± 10.22	118.54 ± 21.26 ***	128.74 ± 11.01 ***

[a] In picomoles per minute per milligram of protein.
[b] In nanomolars.
* $p<0.01$ vs. dSt.
** $p<0.05$ vs. vSt.
*** $p<0.01$ vs. dSt and vSt.

processed for DAT immunocytochemistry, and the numbers of apoptotic nuclei and DAT immunonegative cells were counted.

Statistics

Mathematical analysis was performed using the one-way ANOVA followed by the Tukey honest test for multiple post hoc comparisons. Analysis was performed using the Statistica program (Statsoft; Tulsa, USA). A level of $p<0.05$ was considered as critical for assigning statistical significance. Data are expressed as mean ± standard error of the mean.

Results

Differential expression of glycosylated and non-glycosylated DAT forms in the midbrain and striatum

The use of specific antibodies allowed us to preferentially detect non-glycosylated (immature, 50 kDa) and glycosylated (mature, 75–80 kDa) DAT forms by both Western blot and immunohistochemistry (see Materials and methods). The immunostaining pattern for sc-14002, which detects the 50 kDa band, was preferentially localized in DA cell somata (Fig. 1I), while the pattern for MAB369, which detects the 75 –80 kDa band, was preferentially localized in midbrain DA fibres and striatal terminals (Figs. 1K and L). Besides the distribution pattern based on DAT maturation and traffic to terminals, we found differences in the expression levels of the glycosylated DAT form between different mesostriatal DA cell subpopulations. These differences were evident in midbrain somata as well as striatal terminals of rodents, monkeys, and humans. While the labelling intensity for non-glyco-DAT was similar in DA somata at different dorsoventral levels of the rat SN (Fig. 2A), the labelling intensity for glyco-DAT was higher in those in its ventral tier (SNcv; $p<0.01$, $F=21.2$; Fig. 2B, see also Figs. 1B–D). This difference was also evident in Western blot (Fig. 2C), and confirmed by densitometry, which revealed three-fold higher glyco-DAT expression in DA neurons in the ventral tier (SNcv) than in those in the dorsal tier (SNrm + VTA; $p<0.01$, $F=16.4$; Figs. 2L and M). A similar labelling pattern was found in monkey and human midbrains. As shown in Figs. 2D–K, the labelling intensity for non-glyco-DAT in the human midbrain was similar in DA neurons in the SNcv, SNrm, and VTA (Figs. 2D–G and N), but glyco-DAT levels were 2.2-fold higher in the neurons in the SNcv than in those in the SNrm ($p<0.01$, $F=20.3$) and were 1.6-fold higher in the SNrm neurons than in the neurons in the VTA ($p<0.01$, $F=17.7$; Figs. 2H–K and N).

With respect to the striatum, the labelling intensity for non-glyco-DAT was very similar in the dSt and vSt of mice (Fig. 3A) and rats (data not shown), but glyco-DAT labelling was weaker in the vSt (Fig. 3B), particularly in the accumbens shell and the medial region of the olfactory tubercle of mice, where glyco-DAT expression was virtually undetected (Figs. 3A–C, arrows). In monkeys, no immunostaining differences were observed between both components of the dSt, caudate, and putamen, but the labelling pattern was clearly different in the vSt. While non-glyco-DAT expression was higher than in the dSt, glyco-DAT expression was very faint (Figs. 3D and E, dotted areas). Consequently, the relative expression of both DAT forms (glyco-DAT/non-glyco-DAT index) in the vSt was significantly lower (30%) than in the dSt ($p<0.01$, $F=18.3$; Fig. 3F). As described in rodents, immunolabelling for non-glyco-DAT showed no regional differences in the human striatum (Fig. 3G), but differences became evident in glyco-DAT. The highest glyco-DAT expression levels and glyco-DAT/non-glyco-DAT index were found in the putamen, followed by the caudate nucleus ($p<0.01$ vs. Pu, $F=13.2$), and the lowest ones in the vSt ($p< 0.05$ vs. Ca, $F=7.3$; Figs. 3G–I).

In summary, these data indicate that glyco-DAT expression is higher in soma and terminals of nigrostriatal DA neurons than in those of the mesolimbic DA neurons, suggesting differences in DAT activity between both mesostriatal compartments.

DAT expression and glycosylation in the plasma membrane of striatal terminals correlate with DA uptake

Bearing in mind that DAT activity depends on its localization in the plasma membrane and glycosylation status, we investigated regional differences (dSt vs. vSt) in DAT glycosylation and expression levels in the plasma membrane of striatal synaptosomes, and DA uptake. Western blot of total synaptosomal extracts from rat dSt and vSt showed one band at 75 kDa and another at 50 kDa, indicating the presence of both DAT forms (Fig. 4A, Syn). Western blot of synaptosomal plasma membranes, obtained from avidin-absorbed biotinylated surface proteins or subcellular fractionation, revealed a single band at ~75 kDa (Fig. 4A, Mem), suggesting that the glycosylated form is the only or the predominant DAT variant in DA terminal membranes of both striatal regions. In addition, densitometric analysis using syntaxin (Stx) as a plasma membrane marker, showed that glyco-DAT expression in the plasma membrane of dSt is 2.6-fold higher than in that of the vSt ($p<0.001$, $F=33.1$; Figs. 4B and C).

We next investigated differences in nomifensine-sensitive DA uptake and DAT kinetics between both striatal regions. As shown in Fig. 4D, the high-affinity [^{3}H]DA uptake in dSt synaptosomes was two-fold higher than in those of the vSt ($p<0.001$, $F=29.7$). The kinetics analysis revealed that V_{max} in the dSt was 23% higher than in the vSt ($p<0.01$, $F=13.9$), but K_m was similar in both striatal regions (Table 2 and Fig. 4E). This finding indicates that regional differences in DA uptake depend on the number of uptake sites rather than on DA affinity and agrees with glyco-DAT expression differences between the plasma membrane of both striatal regions. Deglycosylation treatment of synaptosomes caused a significant decrease in [^{3}H]DA uptake (45%–50%; $p<0.001$ deglyco-dSt vs. dSt, $F=37.3$; $p<0.05$ deglyco-vSt vs. vSt, $F=8.0$; Fig. 4D) as well as in both DAT kinetics parameters. K_m was 25%–36% lower after treatment than in untreated striatal synaptosomes, and V_{max} decreased 13%–22% ($p<0.01$, deglyco-dSt vs. dSt, $F=12.7$; $p<0.01$ deglyco-vSt vs. vSt, $F=10.1$; Table 2). These data confirm the key role of glycosylation in DA affinity and that deglycosylation treatment also reduces the number of uptake sites (Fig. 4E).

Fig. 5. Tyrosine hydroxylase immunohistochemistry in the midbrain and striatum of rats (A–D), mice (E–H), monkeys (I–L), and humans (M–Q) showing the topographic pattern of cell and terminal loss in different animal models of PD and in parkinsonian patients. Sham-injected animals are on the left, 6-OHDA- or MPTP-injected animals are in the middle, and human samples (control and parkinsonian brains) on the right. DA cell degeneration in the midbrain of 6-OHDA-injected rats (B), MPTP-injected mice (F) and monkeys (J), and parkinsonian patients (N) mostly involves the SNcv, in agreement with the distribution of DA cells containing high glyco-DAT levels (compare Figs. 2A and B and 5A and B; and Figs. 2D–K and 5M and N). In the striatum of 6-OHDA-injected rats (D) and MPTP-injected mice (H) and monkey (L), the localization of non-degenerate (TH positive) terminals coincides with that of terminals containing low glyco-DAT levels (compare Figs. 3B and 5H; and Figs. 3E and 5L). Moreover, confirming previous anatomical descriptions in PD (Kish et al., 1988; Brooks et al., 1990) and correlating with the glyco-DAT levels, the loss of DA terminals is higher in the putamen than in the caudate nucleus of parkinsonian patients (compare Figs. 3H and 5O–Q). AcS, accumbens shell; Ca, caudate nucleus; dSt, dorsal striatum; EC, external capsule; IC, internal capsule; LV, lateral ventricle; OT, olfactory tubercle; Pu, putamen; SNcv, caudoventrolateral region of the substantia nigra; SNrm, rostrodorsomedial region of the substantia nigra; vSt, ventral striatum; VTA, ventral tegmental area. The dashed line in A, B, I, J, M, and N indicates the putative border between SNrm and SNcv, and in O indicates the putative borders of the internal capsule. Bar in B (for A and B), 400 μm; in D (for C and D), 1 mm; in F (for E and F), 250 μm; in H (for G and H), 400 μm; in J (for I and J), 1 mm; in L (for K and L) 2 mm; in N (for M and N) 2 mm; in O, 6 mm; in Q (for P and Q), 1 mm.

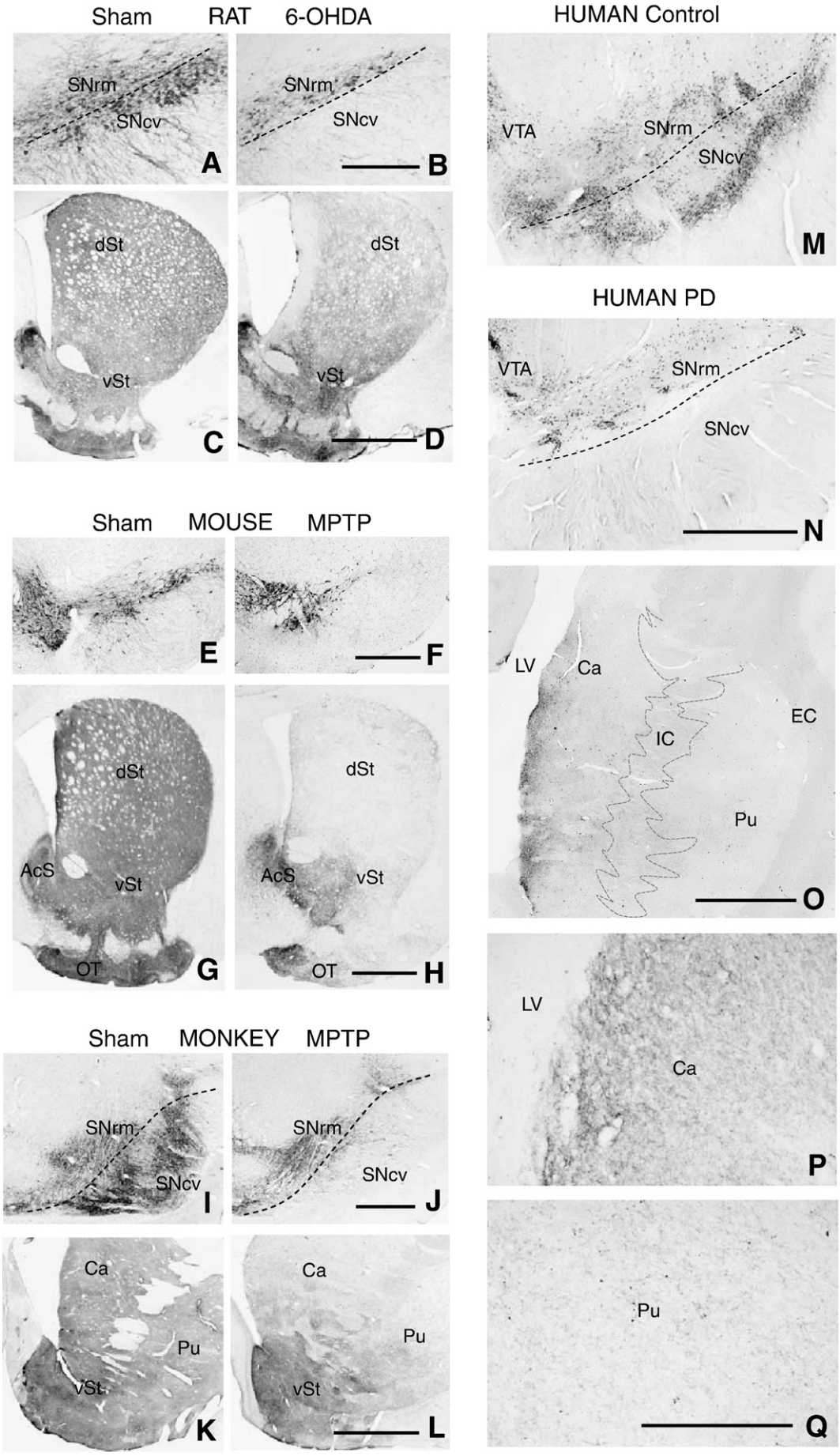
Sham
RAT
6-OHDA
SNrm
SNcv
A
B
dSt
vSt
C
D
Sham
MOUSE
MPTP
E
F
AcS
OT
G
H
Sham
MONKEY
MPTP
I
J
Ca
Pu
K
L
HUMAN Control
VTA
M
HUMAN PD
N
LV
EC
IC
O
P
Q

DAT glycosylation levels positively correlate with DA cell degeneration in animal models of Parkinson's disease and parkinsonian patients

The topographic pattern of glyco-DAT expression was compared with that of DA cell degeneration in three animal models of PD (see Materials and methods) and parkinsonian patients. Immunohistochemistry for tyrosine hydroxylase in rats receiving intracerebroventricular injection of 6-OHDA shows that, coinciding with the distribution of high glyco-DAT level expressing cells, the degeneration is preferentially localized in SNcv somata and dSt terminals (Figs. 5A–D). DA cell degeneration in MPTP-treated mice and monkeys follows the same pattern as in 6-OHDA rats with the loss of practically all SNcv neurons (Figs. 5E, F, I, and J). The field of non-degenerate terminals localizes in the accumbens shell and the medial portion of the olfactory tubercle in the mouse striatum, coinciding with that of terminals containing very low levels of glyco-DAT (compare Fig. 3B with Fig. 5H). Non-degenerated terminals in the striatum of MPTP-treated monkeys are restricted to the vSt, where glyco-DAT levels are very low (compare Figs. 3E and L). Finally, confirming previous anatomical studies in humans (Hassler, 1938; German et al., 1989; Damier et al., 1999b), we found that in the midbrain of parkinsonian patients, DA cells virtually disappear from the SNcv, while many of them in the SNrm and VTA are preserved (Figs. 5M and N). In addition, correlating with glyco-DAT levels in both dSt compartments, the loss of DA terminals was significantly higher in the putamen than in the caudate nucleus (Figs. 5O–Q). These data support a relationship between the constitutive expression of the glycosylated DAT form and the vulnerability of midbrain DA cells against 6-OHDA and MPTP and in PD.

Cytotoxic effect of MPP^+ on glyco-DAT and deglyco-DAT expressing cells

The relationship between DAT glycosylation and the differential vulnerability of DA neurons was confirmed in HEK-293 cells expressing the wild-type form of rat DAT (rDAT) and a mutant form in which two N-glycosylation sites were removed by site-directed mutagenesis (N188Q and N205Q; deglyco-rDAT). Western blot of rDAT stably transfected HEK cells (rDAT-HEK cells) revealed a broad band at 75–80 kDa and a thinner band at 50 kDa (Fig. 6A), corresponding to the glycosylated and non-glycosylated forms, respectively. Low levels of non-glyco-DAT protein expression were detected in non-transfected cells (Fig. 6A) or in cells transfected with the empty vector (data not shown). Endogenous DAT protein levels were not high enough to show significant DA uptake under the experimental conditions used in this study (Fig. 6B) and were not detected by immunofluorescence (Fig. 6D). In contrast, stable transfectants showed an intense labelling preferentially localized in the cell surface (Fig. 6J), and a high degree of activity in the DA uptake assay (Fig. 6B). HEK cells transfected with rDAT mutant form (N188Q and N205Q, deglyco-rDAT-HEK cells) showed one band at ~50 kDa and another at ~60 kDa (Fig. 6A), consistent with the expression of the non-glycosylated and a partially glycosylated DAT variant coming from a third glycosylation site (Torres et al., 2003; Li et al., 2004). Deglyco-rDAT immunofluorescence was reduced in the cell surface (Fig. 6S), and DA uptake was 30% of that in rDAT-HEK cells ($p<0.01$, $F=19.1$; Fig. 6B).

The cytotoxic effects of rotenone and MPP^+ on the different cell phenotypes were studied by using the MTT assay after incubation in rotenone (0.1 –1000 μM) or MPP^+ (0.01 –1000 μM) for 24 hours. The toxicity of rotenone on rDAT- and deglyco-rDAT-HEK cells was similar to that on untransfected HEK cells ($IC_{50}=19$–24 μM) as shown in Fig. 6C. In the case of MPP^+, the toxic effect on untransfected HEK cells was obtained at practically the millimolar concentration range ($IC_{50}=976\pm58$ μM), while in rDAT-HEK cells, it was obtained around 1.0 μM ($IC_{50}=1.33\pm0.29$ μM) and inhibited by coincubation with nomifensine. In contrast, as described for untransfected HEK cells, the effect on deglyco-rDAT HEK cells became evident at the upper range of MPP^+ concentration ($IC_{50}=281\pm39$ μM). The differential response to MPP^+ was confirmed in the morphologic study. After incubation in 50 μM MPP^+ for 24 hours, 47% of rDAT-HEK cells became immunonegative for DAT (Fig. 6M) and 19% of them showed apoptotic nucleus (Fig. 6N). However, no changes were detected in deglyco-rDAT-HEK cells subjected to the same treatment (Fig. 6V) nor in rDAT-HEK cells coincubated with nomifensine (Fig. 6P). These data indicate that DAT deglycosylation reduces DA uptake and protects DAT expressing cells against MPP^+ toxicity and that DAT expression and its glycosylation status do not affect the rotenone toxicity on HEK cells.

Discussion

Our results show differences in the expression of the glycosylated form of DAT among different mesostriatal DA cells and a relatonship between glyco-DAT expression, DA uptake, and vulnerability. DA neurons in the SNcv express higher glyco-DAT levels, transport DA more efficiently, and are more vulnerable to degeneration than those in the SNrm and VTA. The relationship between DAT glycosylation and the differential vulnerability of midbrain DA cells is evident in parkinsonian brains, in three different animal models of PD, and in HEK cells expressing the wild-type form of DAT and a partially glycosylated mutant form.

Previous data from our laboratory suggest internuclear differences in the post-transcriptional processing of DAT. Specifically, midbrain DA cell subsets with similar levels of DAT mRNA showed differences in DAT protein contents (Gonzalez-Hernandez et al., 2004). These results were obtained using an anti-DAT antibody directed to the N-terminal fragment which recognises a ~75 kDa form (Freed et al., 1995; Vaughan et al., 1996). Here, we have used antibodies directed to different fragments of the transporter that identify one form of ~75 kDa and another of ~50 kDa. Previous studies using photoaffinity labelling, enzymatic treatment, and immunological techniques in the identification of the glycosylated and non-glycosylated DAT forms (Grigoriadis et al., 1989; Lew et al., 1991; Patel et al., 1993; Ciliax et al., 1995; Vaughan, 1995), as well as validation tests and immunolabelling differences between different antibodies, indicate that the bands detected at ~75 kDa and 50 kDa correspond to the glycosylated and non-glycosylated DAT forms, respectively. The combination of these antibodies revealed the expected maturational gradient, determined by the evidence of a higher concentration of the non-glycosylated (immature) form in midbrain somata than in striatal terminals, and a higher concentration of the glycosylated (mature) form in striatal terminals than in midbrain somata. Most importantly, they show higher expression levels of glyco-DAT in somata and terminals of the nigrostriatal compartment (SNcv and dSt) than in those of the mesolimbic compartment (SNrm + VTA and vSt). These findings could be secondary to differences in the density of dopaminergic terminals between both striatal regions. However, the fact that differences in glyco-DAT expression were also evident in midbrain somata and that no regional differences were detected at the terminal level in the non-glycosylated DAT form and TH expression make it improbable that structural aspects play a relevant role in this phenomenon and support the existence of differences in the posttranslational processing of DAT between both mesostriatal compartments. Moreover, this expression pattern matches that of the functional DAT pool. DAT levels in the plasma membrane of dSt terminals are higher than in those of the vSt, and only the glycosylated DAT form was detected in the plasma membrane of rat striatal synaptosomes. Consistent with these findings, DA uptake in dSt is higher than in the vSt, and this difference is due to a higher number of DA uptake sites (V_{max} values) without differences in the affinity of DA uptake (K_m values), indicating that expression levels rather than the

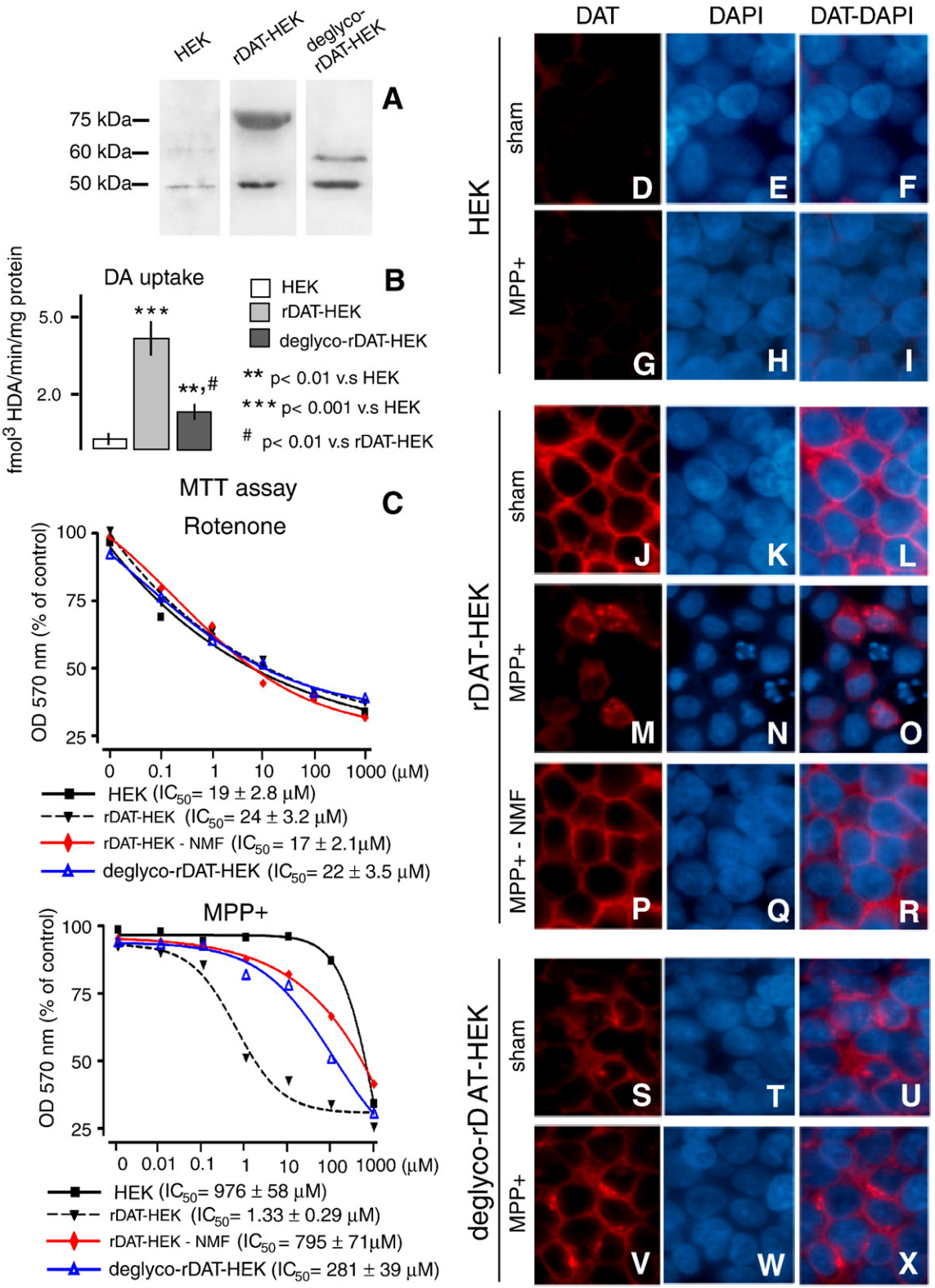

Fig. 6. Cytotoxic effect of MPP^+ and rotenone on HEK-293 cells expressing the wild-type (rDAT) and a partially deglycosylated form (deglyco-rDAT) of rat DAT. (A) Western blot analysis of DAT expression in untransfected cells (HEK) and in cells expressing rDAT (rDAT-HEK) or double mutant (N188Q, N205Q) deglyco-rDAT (deglyco-rDAT-HEK). Untransfected cells show a very weak expression of non-glyco-DAT (50 kDa); rDAT-HEK cells show a robust expression of glyco-DAT (75 kDa); and deglyco-rDAT-HEK cells show a moderate expression of a partially deglyco-DAT form (~60 kDa). (B) DA uptake in deglyco-rDAT-HEK cells is significantly lower than in rDAT-HEK cells. (C) Toxic effect of rotenone (top) and MPP^+ (bottom) on the three cell phenotypes and on rDAT-HEK cells after nomifensine (NMF) treatment measured by MTT reduction. The response to rotenone is similar in the three cell phenotypes. The half-maximal inhibitory concentration of MPP^+ toxicity is much higher in deglyco-rDAT-HEK cells (IC_{50} = 281 μM) than in rDAT-HEK cells (IC_{50} = 1.33 μM). (D–X) Morphological evidence of the differential vulnerability of rDAT-HEK and deglyco-rDAT-HEK cells to MPP^+. Left column, DAT immunocytochemistry; central column, DAPI staining; right column, DAT-DAPI double staining. Cells were incubated with 50 μM MPP^+ for 24 hours. A number of rDAT-HEK cells lost DAT immunoreactivity (M) and displayed apoptotic nuclei (N), but no changes were observed in deglyco-rDAT-HEK cells (V–X), nor in NMF-treated rDAT-HEK (P–R) nor untransfected cells (G–I).

form of the membrane-associated DAT are responsible for DAT activity differences.

The idea that DA uptake is differentially regulated in the dSt and vSt arises from studies reporting that the number of ^{3}H-DA uptake sites in the dSt are higher than in the vSt (Missale et al., 1985; Marshall et al., 1990; Cass et al., 1992), and that after electrical stimulation, the time decline of extracellular DA concentration in the dSt is shorter than in the vSt (Stanford et al., 1988; Suaud-Chagny et al., 1995). Our study shows a relationship between this phenomenon and the glycosylation degree and membrane expression of DAT in both striatal compartments.

It should be noted that although the dSt and vSt receive afferent connections from different brain centres, both regions share relevant aspects of their cytology, local circuitries, and cellular physiology (Leung and Yim, 1993; Meredith, 1999). This suggests that they operate following a common input–output scheme and that the regional specialization should be due to variations in neurochemical parameters (Wickens, 1990). Physiological studies show that DA is involved in long-lasting activity-dependent changes in the excitatory synaptic efficacy, a cellular mechanism required for information storage in different brain regions (Calabresi et al., 2007; Surmeier et al., 2007). In the striatum, DAergic–glutamatergic interaction is believed to underlie motor functions and habit learning associated with the dSt and reward and motivation associated with the vSt (Calabresi et al., 2000; Hyman et al., 2006). The fact that some features of the synaptic changes induced by DA in the dSt are different from those induced in the vSt suggests that the time course of DA signalling might be important in determining their functional specialization (Wickens et al., 2003). In this context, differences in DAT glycosylation and transport rate between nigrostriatal and mesolimbic neurons may act as regulatory mechanisms contributing to shape the pattern of DA time signalling and functional specialization in the dSt and vSt.

On the other hand, several lines of evidence support the view that DAT is involved in DA cell degeneration. DA is an important source of reactive oxygen species (Luo and Roth, 2000; Adams et al., 2001) and the cytosolic levels of DA depend mostly on the DA uptake through DAT (Benoit-Marand et al., 2000). The pharmacological blockade or deficient expression of DAT makes DA cells resistant to dopaminergic neurotoxins (Gainetdinov et al., 1997; Bezard et al., 1999). This relationship has also been supported by the similarity between the distribution pattern of DA cells containing high levels of DAT mRNA and that of DA cell degeneration (Cerruti et al., 1993; Hurd et al., 1994). However, a meticulous analysis of both distribution patterns reveals some inconsistencies. For example, DA cells in the parabrachialis pigmentosus region of the A10 cell group, which contains higher DAT mRNA levels than those in the dorsal tier of SN in monkeys (Haber et al., 1995) and rats (Shimada et al., 1992), are also more resistant to MPTP (Varastet et al., 1994) and 6-OHDA (Rodriguez et al., 2001), respectively. In addition, a comparative study between the mRNA expression pattern of DAT and other dopaminergic markers, including those with a potential protective role such as D_2 receptor (Hurd et al., 1994; Haber et al., 1995) and VMAT2 (Gonzalez-Hernandez et al., 2004), reveals no substantial differences among them, suggesting that the involvement of DAT in the differential vulnerability of DA cells should be related to aspects other than differences in its mRNA levels.

Our study shows a close association between the topographic pattern of glyco-DAT expression and that of mesostriatal degeneration. The distribution of midbrain DA cells, which degenerate in PD, as well as in the 6-OHDA model in rats and the MPTP model in mice and monkeys, coincides with that of DA cells containing high glyco-DAT levels. Glyco-DAT levels in the human striatum are in line with the putamen–caudate–vSt gradient of DA degeneration in parkinsonian patients (Kish et al., 1988; Brooks et al., 1990), and the distribution of 6-OHDA- and MPTP-resistant fibres in the rat, mouse, and monkey striatum coincides with that of glyco-DAT-poor terminals. In any case, it should be noted that other components of the chemical profile of DA cells have also been related to their differential vulnerability in PD. For example, the calcium binding protein calbindin has been proposed as playing a neuroprotective role on the basis of its ability to buffer intracellular Ca^{2+} and the fact that it is preferentially expressed in VTA and SNrm DA cells (Yamada et al., 1990; German et al., 1992). More recently, the use of laser capture microdissection, microarray analysis, and real-time PCR has revealed that more than one hundred genes, some of them involved in vulnerability or neuroprotection, are differentially expressed in DA cells of the SN and VTA of rodents (Chung et al., 2005; Greene et al., 2005). Therefore, phenotypic aspects other than DAT glycosylation may contribute to shape the topographic pattern of DA cell degeneration in PD.

In order to confirm the anatomical suggestion of a relationship between DAT glycosylation and DA cell vulnerability, *in vitro* experiments were performed. We used a cell model similar to that used to demonstrate the relevance of N-glycosylation in DAT activity (Torres et al., 2003; Li et al., 2004), but substituting human DAT for rat DAT because both forms display the same activity and susceptibility to MPP^+ in transfected cells (Pifl et al., 1993). The double mutation N188Q and N205Q resulted in partial deglycosylation of DAT, reduced DAT immunoreactivity at the plasma membrane, and reduced DA uptake. The *in vitro* results support those obtained in rat striatal synaptosomes showing a correlation between glyco-DAT expression and DA uptake, the differences in glyco-DAT expression between dSt and vSt, and the effect of deglycosylation. In addition, DAT transfection and mutation were sensitive to DAT-dependent neurotoxins but not to DAT-independent neurotoxins. The cytotoxic assay reproduced the vulnerability differences found between SNcv and SNrm + VTA DA cells in PD and in 6-OHDA and MPTP models of PD, with rDAT-HEK cells being highly sensitive to MPP^+, while those expressing the deglycosylated DAT form are resistant.

Glycosylation is a co- and posttranslational process that engages numerous enzymes which add glycans to newly synthesized proteins, with enzymes working in DAT glycosylation also being used in the glycosylation of other membrane-associated proteins (Melikian et al., 1996; Helenius and Aebi, 2001). Therefore, it is unlikely that internuclear differences (SNcv vs. SNrm + VTA) in DAT glycosylation are due to differences in the enzymatic phenotype of DA cells, since this would affect the surface expression of other important proteins. Several studies indicate that other factors modulate DAT membrane expression and activity, including D_2 and D_3 DA receptor activation (Cass and Gerhardt, 1994; Joyce et al., 2004), and direct interaction with various presynaptic proteins (Torres et al., 2001). Although many functional aspects of these interactions remain unknown, it is possible that they can also modulate the glycosylation status of DAT.

Taken together, our results strongly suggest that the glycosylation status of DAT is involved in the degeneration of DA cells in PD. Further studies focused on the differential modulation of DAT glycosylation and trafficking between mesostriatal subpopulations may contribute to understanding the mechanisms underlying this relationship.

Acknowledgments

This work was supported by Ministerio de Ciencia e Innovación (grant no. BFU2007-66561), Fundación Canaria de Invetigación y Salud (grant no. 71/07), CIBERNED (ISCIII), and Instituto de Tecnologías Biomédicas.

Appendix A. Supplementary data

Supplementary data associated with this article can be found, in the online version, at doi:10.1016/j.nbd.2009.09.002.

References

Adams Jr., J.D., Chang, M.L., Klaidman, L., 2001. Parkinson's disease—redox mechanisms. Curr. Med. Chem. 8, 809–814.

Benoit-Marand, M., Jaber, M., Gonon, F., 2000. Release and elimination of dopamine in vivo in mice lacking the dopamine transporter: functional consequences. Eur. J. Neurosci. 12, 2985–2992.
Bernheimer, H., Birkmayer, W., Hornykiewicz, O., Jellinger, K., Seitelberger, F., 1973. Brain dopamine and the syndromes of Parkinson and Huntington. Clinical, morphological and neurochemical correlations. J. Neurol. Sci. 20, 415–455.
Bezard, E., Gross, C.E., Fournier, M.C., Dovero, S., Bloch, B., Jaber, M., 1999. Absence of MPTP-induced neuronal death in mice lacking the dopamine transporter. Exp. Neurol. 155, 268–273.
Blum, D., Torch, S., Lambeng, N., Nissou, M., Benabid, A.L., Sadoul, R., Verna, J.M., 2001. Molecular pathways involved in the neurotoxicity of 6-OHDA, dopamine and MPTP: contribution to the apoptotic theory in Parkinson's disease. Prog. Neurobiol. 65, 135–172.
Braak, H., Del Tredici, L., Rüb, U., de Vos, R.A., Jansen Steur, E.N., Braak, E., 2003. Staging of brain pathology related to sporadic Parkinson's disease. Neurobiol. Aging 24, 197–211.
Brooks, D.J., Ibanez, V., Sawle, G.V., Quinn, N., Lees, A.J., Mathias, C.J., Bannister, R., Marsden, C.D., Frackowiak, R.S., 1990. Differing patterns of striatal ^{18}F-DOPA uptake in Parkinson's disease, multiple system atrophy, and progressive supranuclear palsy. Ann. Neurol. 28, 547–555.
Burns, R.S., Chiueh, C.C., Markey, S.P., Ebert, M.H., Jacobowitz, D.M., Kopin, I.J., 1983. A primate model of parkinsonism: selective destruction of dopaminergic neurons in the pars compacta of the substantia nigra by *N*-methyl-4-phenyl-1,2,3,6-tetrahydropyridine. Proc. Natl. Acad. Sci. U. S. A. 80, 4546–4550.
Burke, R.E., Dauer, W.T., Vonsattel, J.P.G., 2008. A critical evaluation of the Braak staining scheme for Parkinson's disease. Ann. Neurol. 64, 485–491.
Calabresi, P., Centonze, D., Gubellini, P., Marfia, G.A., Pisani, A., Sancesario, G., Bernardi, G., 2000. Synaptic transmission in the striatum: from plasticity to neurodegeneration. Prog. Neurobiol. 61, 231–265.
Calabresi, P., Picconi, B., Tozzi, A., Di Filippo, M., 2007. Dopamine-mediated regulation of corticostriatal synaptic plasticity. Trends Neurosci. 30, 211–219.
Cass, W.A., Gerhardt, G.A., 1994. Direct in vivo evidence that D_2 dopamine receptors can modulate dopamine uptake. Neurosci. Lett. 176, 259–263.
Cass, W.A., Gerhardt, G.A., Mayfield, R.D., Curella, P., Zahniser, N.R., 1992. Differences in dopamine clearance and diffusion in rat striatum and nucleus accumbens following systemic cocaine administration. J. Neurochem. 59, 259–266.
Caudle, W.M., Colebrooke, R.E., Emson, P.C., Miller, G.W., 2008. Altered vesicular dopamine storage in Parkinson's disease: a premature demise. Trends Neurosci. 31, 3003–3308.
Cerruti, C., Walther, D.M., Kuhar, M.J., Uhl, G.R., 1993. Dopamine transporter mRNA expression is intense in rat midbrain neurons and modest outside midbrain. Brain Res. Mol. Brain Res. 18, 181–186.
Chung, C.Y., Seo, H., Sonntag, K.C., Brooks, A., Lin, L., Isacson, O., 2005. Cell type-specific gene expression of midbrain dopaminergic neurons reveals molecules involved in their vulnerability and protection. Hum. Mol. Genet. 14, 1709–1725.
Ciliax, B.J., Heilman, C., Demchyshyn, L.L., Pristupa, Z.B., Ince, E., Hersch, S.M., Niznik, H.B., Levey, A.I., 1995. The dopamine transporter: immunochemical characterization and localization in brain. J. Neurosci. 15, 1714–1723.
Cruz-Muros, I., Afonso-Oramas, D., Abreu, P., Pérez-Delgado, M.M., Rodriguez, M., Gonzalez-Hernandez, T., 2009. Aging effects on the dopamine transporter expression and compensatory mechanisms. Neurobiol. Aging 30, 973–986.
Dahlström, A., Fuxe, K., 1964. Evidence for the existence of monoamine-containing neurons in the central nervous system: I. Demonstration of monoamines in the cell bodies of brain stem neurons. Acta Physiol. Scand. 62 (Suppl. 232), 1–55.
Damier, P., Hirsch, E.C., Agid, Y., Graybiel, A.M., 1999a. The substantia nigra of the human brain: I. Nigrosomes and the nigral matrix, a compartmental organization based on calbindin D(28K) immunohistochemistry. Brain 122 (Pt. 8), 1421–1436.
Damier, P., Hirsch, E.C., Agid, Y., Graybiel, A.M., 1999b. The substantia nigra of the human brain: II. Patterns of loss of dopamine-containing neurons in Parkinson's disease. Brain 122 (Pt. 8), 1437–1448.
Dunah, A.W., Standaert, D.G., 2001. Dopamine D_1 receptor-dependent trafficking of striatal NMDA glutamate receptors to the postsynaptic membrane. J. Neurosci. 21, 5546–5558.
Elbaz, A., Moisan, F., 2008. Update in the epidemiology of Parkinson's disease. Curr. Opin. Neurol. 21, 454–460.
Fallon, J.H., Loughlin, S.E., 1982. Monoamine innervation of the forebrain: collateralization. Brain Res. Bull. 9, 295–307.
Foix, C., Nicolescom, J., 1925. Anatomie cérébrale. Les noyaux gris centraux et la región Mésencéphalo-sous-optique. Suivi d'un apéndice sur l'anatomie pathologique de la maladie de Parkinson. Masson et Cie, Paris, pp. 508–538.
Freed, C., Revay, R., Vaughan, R.A., Kriek, E., Grant, S., Uhl, GR., Kuhar, M.J., 1995. Dopamine transporter immunoreactivity in rat brain. J. Comp. Neurol. 359, 340–349.
Gainetdinov, R.R., Fumagalli, F., Jones, S.R., Caron, M.G., 1997. Dopamine transporter is required for in vivo MPTP neurotoxicity: evidence from mice lacking the transporter. J. Neurochem. 69, 1322–1325.
German, D.C., Manaye, K., Smith, W.K., Woodward, D.J., Saper, C.B., 1989. Midbrain dopaminergic cell loss in Parkinson's disease: computer visualization. Ann. Neurol. 26, 507–514.
German, D.C., Manaye, K.F., Sonsalla, P.K., Brooks, B.A., 1992. Midbrain dopaminergic cell loss in Parkinson's disease and MPTP-induced parkinsonism: sparing of calbindin-D28k-containing cells. Ann. N.Y. Acad. Sci. 648, 42–62.
Giros, B., Caron, M.G., 1993. Molecular characterization of the dopamine transporter. Trends Pharmacol. Sci. 14, 43–49.
Gonzalez-Hernandez, T., Barroso-Chinea, P., De La Cruz-Muros, I., Perez-Delgado, M.M., Rodriguez, M., 2004. Expression of dopamine and vesicular monoamine transporters and differential vulnerability of mesostriatal dopaminergic neurons. J. Comp. Neurol. 479, 198–215.
Greene, J.G., Dingledine, R., Greenamyre, J.T., 2005. Gene expression profiling of rat midbrain dopamine neurons: implications for selective vulnerability in parkinsonism. Neurobiol. Dis. 18, 19–31.
Grigoriadis, D.E., Wilson, A.A., Lew, R., Sharkey, J.S., Kuhar, M.J., 1989. Dopamine transport sites selectively labeled by a novel photoaffinity probe: ^{125}I-DEEP. J. Neurosci. 9, 2664–2670.
Haber, S.N., Ryoo, H., Cox, C., Lu, W., 1995. Subsets of midbrain dopaminergic neurons in monkeys are distinguished by different levels of mRNA for the dopamine transporter: comparison with the mRNA for the D_2 receptor, tyrosine hydroxylase and calbindin immunoreactivity. J. Comp. Neurol. 362, 400–410.
Hassler, R., 1938. Zur pathologie der paralysis agitans und des postencephalitschen Parkinsonismus. J. Psychol. Neurol. 48, 387–476.
Heimer, L., 2003. A new anatomical framework for neuropsychiatric disorders and drug abuse. Am. J. Psychiatry 160, 1726–1739.
Helenius, A., Aebi, M., 2001. Intracellular functions of N-linked glycans. Science 291, 2364–2369.
Hirsch, E., Graybiel, A.M., Agid, Y.A., 1988. Melanized dopaminergic neurons are differentially susceptible to degeneration in Parkinson's disease. Nature 334, 345–348.
Horn, A.S., 1990. Dopamine uptake: a review of progress in the last decade. Prog. Neurobiol. 34, 387–400.
Hung, H.C., Lee, E.H., 1996. The mesolimbic dopaminergic pathway is more resistant than the nigrostriatal dopaminergic pathway to MPTP and MPP^+ toxicity: role of BDNF gene expression. Brain Res. Mol. Brain Res. 41, 14–26.
Hurd, Y.L., Pristupa, Z.B., Herman, M.M., Niznik, H.B., Kleinman, J.E., 1994. The dopamine transporter and dopamine D_2 receptor messenger RNAs are differentially expressed in limbic- and motor-related subpopulations of human mesencephalic neurons. Neuroscience 63, 357–362.
Huttner, W.B., Schiebler, W., Greengard, P., De Camilli, P., 1983. Synapsin I (protein I), a nerve terminal-specific phosphoprotein: III. Its association with synaptic vesicles studied in a highly purified synaptic vesicle preparation. J. Cell Biol. 96, 1374–1388.
Hyman, S.E., Malenka, R.C., Nestler, E.J., 2006. Neural mechanisms of addiction: the role of reward-related learning and memory. Ann. Rev. Neurosci. 29, 565–598.
Jackson-Lewis, V., Jakowec, M., Burke, R.E., Przedborski, S., 1995. Time course and morphology of dopaminergic neuronal death caused by the neurotoxin 1-methyl-4-phenyl-1,2,3,6-tetrahydropyridine. Neurodegeneration 4, 257–269.
Jenner, P., Olanow, C.W., 2006. The pathogenesis of cell death in Parkinson's disease. Neurology 66, S24–S36.
Joel, D., Weiner, I., 2000. The connections of the dopaminergic system with the striatum in rats and primates: an analysis with respect to the functional and compartmental organization of the striatum. Neuroscience 96, 451–474.
Joyce, J.N., Woolsey, C., Ryoo, H., Borwege, S., Hagner, D., 2004. Low dose pramipexole is neuroprotective in the MPTP mouse model of Parkinson's disease, and down-regulates the dopamine transporter via the D_3 receptor. BMC Biol. 2, 22.
Kish, S.J., Shannak, K., Hornykiewicz, O., 1988. Uneven pattern of dopamine loss in the striatum of patients with idiopathic Parkinson's disease. Pathophysiologic and clinical implications. N. Engl. J. Med. 318, 876–880.
Kubis, N., Faucheux, B.A., Ransmayr, G., Damier, P., Duyckaerts, C., Henin, D., Forette, B., Le Charpentier, Y., Hauw, J.J., Agid, Y., Hirsch, E.C., 2000. Preservation of midbrain catecholaminergic neurons in very old human subjects. Brain 123 (Pt. 2), 366–373.
Kukuruzinska, M.A., Lennon, K., 1998. Protein N-glycosylation: molecular genetics and functional significance. Crit. Rev. Oral Biol. Med. 9, 415–448.
Kurlan, R., Kim, M.H., Gash, D.M., 1991. Oral levodopa dose–response study in MPTP-induced hemiparkinsonian monkeys: assessment with a new rating scale for monkey parkinsonism. Mov. Disord. 6, 111–118.
Lee, F.J., Liu, F., 2008. Genetic factors involved in the pathogenesis of Parkinson's disease. Brain Res. Rev. 58, 354–364.
Leung, L.S., Yim, C.Y., 1993. Rhythmic delta-frequency activities in the nucleus accumbens of anesthetized and freely moving rats. Can. J. Physiol. Pharmacol. 71, 311–320.
Lew, R., Grigoriadis, D., Wilson, A., Boja, J.W., Simantov, R., Kuhar, M.J., 1991. Dopamine transporter: deglycosylation with exo- and endoglycosidases. Brain Res. 539, 239–246.
Li, L.B., Chen, N., Ramamoorthy, S., Chi, L., Cui, X.N., Wang, L.C., Reith, M.E., 2004. The role of N-glycosylation in function and surface trafficking of the human dopamine transporter. J. Biol. Chem. 279, 21012–21020.
Lis, H., Sharon, N., 1993. Protein glycosylation. Structural and functional aspects. Eur. J. Biochem. 218, 1–27.
Luo, Y., Roth, G.S., 2000. The roles of dopamine oxidative stress and dopamine receptor signaling in aging and age-related neurodegeneration. Antioxid. Redox Signal 2, 449–460.
Marshall, J.F., O'Dell, S.J., Navarrete, R., Rosenstein, A.J., 1990. Dopamine high-affinity transport site topography in rat brain: major differences between dorsal and ventral striatum. Neuroscience 37, 11–21.
Melikian, H.E., Ramamoorthy, S., Tate, C.G., Blakely, R.D., 1996. Inability to N-glycosylate the human norepinephrine transporter reduces protein stability, surface trafficking, and transport activity but not ligand recognition. Mol. Pharmacol. 50, 266–276.
Meredith, G.E., 1999. The synaptic framework of chemical signaling in nucleus accumbens. Ann. N.Y. Acad. Sci. 877, 140–156.
Miller, G.W., Staley, J.K., Heilman, C.J., Perez, J.T., Mash, D.C., Rye, D.B., Levey, A.I., 1997. Immunochemical analysis of dopamine transporter protein in Parkinson's disease. Ann. Neurol. 41, 530–539.
Miller, G.W., Gainetdinov, R.R., Levey, A.I., Caron, M.G., 1999. Dopamine transporters and neuronal injury. Trends Pharmacol. Sci. 20, 424–429.
Missale, C., Castelletti, L., Govoni, S., Spano, P.F., Trabucchi, M., Hanbauer, I., 1985.

Dopamine uptake is differentially regulated in rat striatum and nucleus accumbens. J. Neurochem. 45, 51–56.
Patel, A., Uhl, G., Kuhar, M.J., 1993. Species differences in dopamine transporters: postmortem changes and glycosylation differences. J. Neurochem. 61, 496–500.
Paxinos, G., Watson, C., 1998. The Rat Brain in Stereotaxic Coordinates. Academic Press, Orlando.
Pifl, C., Giros, B., Caron, M.G., 1993. Dopamine transporter expression confers cytotoxicity to low doses of the parkinsonism-inducing neurotoxin 1-methyl-4-phenylpyridinium. J. Neurosci. 13, 4246–4253.
Rodriguez, M., Barroso-Chinea, P., Abdala, P., Obeso, J., Gonzalez-Hernandez, T., 2001. Dopamine cell degeneration induced by intraventricular administration of 6-hydroxydopamine in the rat: similarities with cell loss in Parkinson's disease. Exp. Neurol. 169, 163–181.
Salvatore, M.F., Apparsundaram, S., Gerhardt, G.A., 2003. Decreased plasma membrane expression of striatal dopamine transporter in aging. Neurobiol. Aging 24, 1147–1154.
Schober, A., 2004. Classic toxin-induced animal models of Parkinson's disease: 6-OHDA and MPTP. Cell Tissue Res. 318, 215–224.
Schott, B.H., Seidenbecher, C.I., Fenker, D.B., Lauer, C.J., Bunzeck, N., Bernstein, H.G., Tischmeyer, W., Guldenfinger, E.D., Heinze, H.J., Duzel, E., 2006. The dopaminergic midbrain participates in human episodic memory formation: evidence from genetic imaging. J. Neurosci. 26, 1407–1417.
Shimada, S., Kitayama, S., Walther, D., Uhl, G., 1992. Dopamine transporter mRNA: dense expression in ventral midbrain neurons. Brain Res. Mol. Brain Res. 13, 359–362.
Stanford, J.A., Kruk, Z.L., Palij, P., Millar, J., 1988. Diffusion and uptake of dopamine in rat caudate and nucleus accumbens compared using fast cyclic voltammetry. Brain Res. 448, 381–385.
Storch, A., Ludolph, A.C., Schwarz, J., 2004. Dopamine transporter: involvement in selective dopaminergic neurotoxicity and degeneration. J. Neural Transm. 111, 1267–1286.
Suaud-Chagny, M.K., Dugast, C., Chergui, K., Msghina, M., Gonon, G., 1995. Uptake of dopamine released by impulses flow in the rat mesolimbic and striatal system in vivo. J. Neurochem. 65, 2603–2611.
Surmeier, D.J., Ding, J., Day, M., Wang, Z., Shen, W., 2007. D_1 and D_2 dopamine-receptor modulation of striatal glutamatergic signaling in striatal medium spiny neurons. Trends Neurosci. 30, 228–235.
Torres, G.E., Yao, W.D., Mohn, A.R., Quan, H., Kim, K.M., Levey, A.I., Staudinger, J., Caron, M.G., 2001. Functional interaction between monoamine plasma membrane transporters and the synaptic PDZ domain-containing protein PICK1. Neuron 30, 121–134.
Torres, G.E., Carneiro, A., Seamans, K., Fiorentini, C., Sweeney, A., Yao, W.D., Caron, M.G., 2003. Oligomerization and trafficking of the human dopamine transporter. Mutational analysis identifies critical domains important for the functional expression of the transporter. J. Biol. Chem. 278, 2731–2739.
Uhl, G.R., Walther, D., Mash, D., Faucheux, B., Javoy-Agid, F., 1994. Dopamine transporter messenger RNA in Parkinson's disease and control substantia nigra neurons. Ann. Neurol. 35, 494–498.
Uversky, V.N., 2004. Neurotoxicant-induced animal models of Parkinson's disease: understanding the role of rotenone, maneb and paraquat in neurodegeneration. Cell Tissue Res. 381, 225–241.
Varastet, M., Riche, D., Maziere, M., Hantraye, P., 1994. Chronic MPTP treatment reproduces in baboons the differential vulnerability of mesencephalic dopaminergic neurons observed in Parkinson's disease. Neuroscience 63, 47–56.
Vaughan, R.A., 1995. Photoaffinity-labeled ligand binding domains on dopamine transporters identified by peptide mapping. Mol. Pharmacol. 47, 956–964.
Vaughan, R.A., Brown, V.L., McCoy, M.T., Kuhar, M.J., 1996. Species- and brain region-specific dopamine transporters: immunological and glycosylation characteristics. J. Neurochem. 66, 2146–2152.
Wickens, J.R., 1990. Striatal dopamine in motor activation and reward-mediated learning. Steps towards a unifying model. J. Neural Transm. 80, 9–30.
Wickens, J.R., Christopher, S.B., Hyland, B.I., Arbuthnott, G.W., 2003. Striatal contributions to reward and decision making. Making sense of regional variations in a reiterated processing matrix. Curr. Opin. Neurobiol. 13, 685–690.
Yamada, T., McGeer, P.L., Baimbridge, K.G., McGeer, E.G., 1990. Relative sparing in Parkinson's disease of substantia nigra dopamine neurons containing calbindin-D28K. Brain Res 526, 303–307.
Zaleska, M.M., Erecinska, M., 1987. Involvement of sialic acid in high-affinity uptake of dopamine by synaptosomes from rat brain. Neurosci. Lett. 82, 107–112.
Zhu, J., Apparsundaram, S., Bardo, M.T., Dwoskin, L.P., 2005. Environmental enrichment decreases cell surface expression of the dopamine transporter in rat medial prefrontal cortex. J. Neurochem. 93, 1434–1443.